Grapevine phyllosphere pan-metagenomics reveals pan-microbiome structure, diversity, and functional roles in downy mildew resistance

Jingyun Jin[1], Xiangfeng Wang[1], Xuenan Zhang[1], Junjie Mei[1], Wei Zheng[1], Linling Guo[1], Haisheng Sun[1], Lili Zhang[1], Chonghuai Liu[2], Wenxiu Ye[1]* and Li Guo[1]*

1. Peking University Institute of Advanced Agricultural Sciences, Shandong Laboratory of Advanced Agricultural Sciences in Weifang, Shandong 261325, China.

2. Zhengzhou Fruit Research Institute, Chinese Academy of Agricultural Sciences, Zhengzhou 450004, China.

*Corresponding author: wenxiu.ye@pku-iaas.edu.cn, li.guo@pku-iaas.edu.cn

Abstract

Grapevines are among the most economically important fruit crops, and microbiome profoundly influence their health, yield, and quality. However, mechanistic insights into microbiome-orchestrated grapevine biology remain limited. Here, we conduct large-scale pan-metagenomic and pan-metatranscriptomic analyses of the phyllosphere microbiome from 107 grapevine accessions spanning 34 *Vitis* species. We show that the grapevine core microbiome is dominated by phylum Bacillota and Pseudomonadota. Leveraging HiFi long-read sequencing technology, we assembled 19 high-quality metagenome-assembled genomes (MAGs) from the grapevine pan-microbiome, representing the first MAG

reconstruction in plant-associated microbial communities using HiFi long reads. These MAGs encode genes associated with antibiotic resistance, secondary metabolism, and carbohydrate-active enzymes (CAZymes), which could potentially influence grapevine biology. During downy mildew (DM) infection, DM-resistant grapevines exhibit significantly higher microbial network complexity than susceptible counterparts. Among the key taxa contributing to this complexity, Bacillota emerged as the dominant phylum with displaying strong abundance correlations with phylum Euglenozoa and Cyanobacteriota, and an isolated Bacillota species from the grapevine leaves, *Bacillus cereus*, demonstrated potent biocontrol activity against DM infection. Pan-metatranscriptomic analysis further revealed significant upregulation of eukaryotic microbial genes involved in primary and secondary metabolism. This pan-metagenomic study offers unprecedented insights into the complex structure, diversity and functional roles of grapevine phyllosphere microbiome, and presents valuable genomic and microbial resources for microbiome research and engineering to enhance viticulture productivity and quality.

Introduction

Grapevines are perennial plants belonging to Vitaceae family renowned for their exceptional flavor as well as their significant economic and nutritional value. In 2023, global grape production reached 72 million tons, with China, Italy, France leading as the top producers, and the global production value of grapes was estimated at 92 billion USD [1]. In addition, grapes are rich in bioactive compounds, including polyphenols, phenolic acids, vitamins,

and dietary fiber, which provide a variety of health benefits, such as anticancer, antidiabetic, cardioprotective, and gut-microbiome-regulating properties [2]. Despite remarkable advancements in grape breeding and cultivation in recent decades, grape production worldwide remains significantly threatened by diseases such as downy mildew (DM), powdery mildew, and gray mold, causing substantial economic losses across grape productions and related industries each year [3–7]. Especially, DM is the most destructive among the diseases that caused by the oomycete *Plasmopara viticola*, severely affecting grape production and quality by causing damages on leaves and fruit clusters [8]. To address these challenges, it is crucial to investigate grapevine-associated microbiome, which could serve as a foundation for developing environmentally friendly and sustainable microbiome-based biocontrol methods in viticulture.

Microbiome, often regarded as the second genome of plants, plays crucial roles in nutrient absorption, disease resistance, and overall plant health [4]. Microbiome profoundly affects grape productivity and the quality of grape-derived products such as wine and raisins [9–11]. The grapevine microbiome primarily consists of bacteria and fungi, with Actinomycetota, Bacillota, and Pseudomonadota being the most prevalent phyla, based on previous 16s rRNA amplicon sequencing [4]. The microbiome composition varies across grapevine tissues with the highest microbial diversity observed in roots and gradually decreasing for trunks and leaves [4]. Studies show that grapevine genetic backgrounds and geographic origins are primary factors influencing their microbial compositions [9,12–20]. Despite the advancement, current plant microbiome studies primarily rely on 16S rRNA sequencing which yields limited insights into mechanistic understanding of microbiome

functions compared to shotgun metagenomics using next-generation sequencing (NGS). However, NGS-based metagenomics falls short in assembling the complete microbial genomes given the limitation of short reads, impeding accurate annotations and functional analysis of metagenome. So far, long-read technologies mainly have been used in microbiome studies for human related samples [21,22], but remain underutilized in plant and agricultural metagenomics. In addition, metatranscriptomics, which crucial to understanding functional implications of microbiome by revealing microbiome gene expression changes, has not been widely adopted in plant microbiome research. Most importantly, integrating pan-metagenomics and pan-metatranscriptomics of plants to study the diversity of microbial profiles across plant species and cultivars have not been reported. These limitations hinder the exploration of grapevine microbiome and the application of microbial biocontrol in viticulture.

Here, we conducted a comprehensive pan-metagenomic analysis of grapevine leaves from 107 *Vitis* accessions (each accession corresponds to a unique *Vitis* cultivar, except for a few samples) spanning 34 species, utilizing NGS, HiFi, RNA-seq data and DM resistance phenome data. Through systematic profiling of the grapevine phyllosphere microbiome, we identified dominant microbial communities under pan-metagenomic framework. Leveraging HiFi reads, we successfully generated 19 high-quality grapevine phyllospheric metagenome-assembled genomes (GPMAGs), and comprehensively annotated genes associated with antibiotic resistance, secondary metabolism, and CAZymes. Based on the phenome data, we revealed that the microbiome from DM-resistant grapevines exhibit significantly more complex microbial networks than susceptible ones. Additionally, we

identified key genera potentially conferring resistance to DM infection, with Bacillota emerging as the dominant phylum exhibiting high abundance correlation with Euglenozoa and Cyanobacteriota, and experimentally validated the potent biocontrol activity of two *Bacillus cereus* strains against DM. Pan-metatranscriptomic analysis further highlighted significant changes in the expression of eukaryotic primary and secondary metabolism genes in response to DM infection. These findings provide novel insights into grapevine microbiome and valuable genomic and microbial resources for viticulture, laying a solid foundation for developing microbiome-based strategies to enhance grape health and promote sustainable production.

Results

Grapevine core microbiome is dominated by Bacillota and Pseudomonadota

To investigate the microbiome profile of the grapevine phyllosphere across grapevines, we collected a total of 107 leaf samples from 34 *Vitis* species covering 100 grapevine cultivars originated from various geographical locations with distinct genotypes and DM resistances [23] (**Fig. 1a, b and Table S1**), and conducted pan-metagenomic analysis as outlined in the workflow (**Fig. 1c**). The metagenomes of the samples were sequenced using Illumina paired-end sequencing [23], yielding a total of 107 NGS datasets (**Fig. 1d**). The reads belonging to the grapevines were completely filtered out by mapping against a complete grapevine genome [23] (VHP-T2T.hap1, NCBI accession: GCA_046255155.1) (**Table S2**), with on average 4.4 million microbial reads remaining per sample. Taxonomic classification

of these microbial reads using Kraken2 [24] identified a total of 1,326 genera across the grapevine phyllosphere (**Fig. 2a and Table S3**). Among these, Bacillota (43.6%) and Pseudomonadota (37.9%) dominated the microbiome profile at the phylum level, while *Lactiplantibacillus* (42.1%) and *Xanthomonas* (22.2%) were the two most abundant genera (**Fig. 2b**). Furthermore, kingdom-level profiling demonstrated that bacteria dominated the grapevine microbiome (91.3%), and other kingdoms accounted for less than 10% (**Fig. 2c**). Notably, the non-bacterial kingdoms exhibited single dominating phyla, such as Euryarchaeota dominating Archaea, Ascomycota and Euglenozoa dominating Eukaryota, and Cressdnaviricota dominating viruses, reflecting specific phylum preference of the grapevine microbiome. To examine worldwide representativeness of our microbial composition, we analyzed worldwide representative accessions from published NGS data containing a global grapevine phyllosphere collection [25] using the same bioinformatic pipeline. The phylum-level microbial composition of the global microbiome generally consistent with our NGS-based composition (**Fig. S1**), demonstrating the worldwide representativeness of our microbial composition. These results highlight the prevalence of Bacillota and Pseudomonadota and their potential roles in the grapevine microbiome.

Although several previous studies have profiled grapevine microbiomes [9,12–20], mostly using 16S rDNA amplicon sequencing, a comprehensive pan-metagenomic analysis leveraging large-scale NGS datasets had not been conducted prior to this study, which could provide critical insights into the structure and functional roles of grapevine microbiome. Through our pan-metagenomic analysis of 107 grapevine phyllosphere, we identified seven core genera (present in all accessions), 945 dispensable genera (present in some but not all

accessions), and 374 unique genera (exclusive to a single accession) based on presence and absence patterns (**Fig. 2d and Table S3**). Strikingly, although the core microbiome accounted for only 0.6% of the detected genera, it dominated 77.3% of the relative abundance, with Bacillota (55.2%) and Pseudomonadota (44.0%) as the major phyla in the core microbiome (**Fig. 2e**). This result further underscores the central role of the core microbiome (mainly Bacillota and Pseudomonadota) in shaping the grapevine phyllosphere microbiome.

Assembly of grapevine phyllospheric metagenome-assembled genomes (GPMAGs)

To assemble high-quality GPMAGs that provide further insights into the potential functions of the grapevine phyllosphere microbiome that potentially influence the host's biology, we generated a total of 103 HiFi long-read sequencing datasets [23] (**Fig. 1d**) for the grapevine accessions used in NGS-based metagenomic analysis above. The HiFi reads were mapped against the grapevine reference genome to completely exclude host-derived sequences, retaining unmapped reads representing microbial data (**Table S2**). These unmapped reads from all accessions were pooled together and then assembled into contigs by using various assemblers, such as Flye [26], hifiasm [27], hifiasm-meta [28], metaFlye [29], metaMDBG [30], and Verkko [31]. The contigs were subsequently binned using CONCOCT [32], Maxbin 2.0 [33], MetaBAT 2 [34], followed by dereplication with Galah (https://github.com/wwood/galah). This workflow generated a total of 19 non-redundant GPMAGs (**Fig. 3a and Table S4**) that met the medium-quality threshold based on standard

MAG quality assessment criteria [30]. Among these, four were classified as complete, three as near-complete, five as high-quality, and seven as medium-quality MAGs (**Fig. 3b and Table S4**), highlighting the high quality of the GPMAGs. The median genome size of the GPMAGs were 4.5 Mb for the complete, 4.6 Mb for the near-complete, 4.7 Mb for the high-quality, 4.2 Mb for the medium-quality (**Fig. 3c and Table S4**), approximating typical bacterial genome sizes. Subsequently, GTDB-tk [35] was employed to identify the microbial profile of the GPMAGs. Among the classified GPMAGs, 63.2 % belonged to Pseudomonadota, 5.3% to Bacillota, and 21.1% to Actinomycetota (**Fig. 3d and Table S4**), which generally aligned with the NGS-based microbial composition (**Fig. 2b**), except for Bacillota. To examine the pan-genomic profile of the GPMAGs among the different HiFi accessions, we further investigated the relevance of the GPMAG with the different grapevine accessions measured by the HiFi read mapping rates against each GPMAGs. Across the grapevine accessions, *Mangrovibacter phragmitis* exhibited the highest relevance, followed by *Roseateles* and *Sphingomonas aquatilis* and (**Fig. 3e**). Interestingly, these GPMAGs all belonged to Pseudomonadota, further supporting its prevalence across grapevine accessions as indicated by the NGS-based microbial composition (**Fig. 2b**). Moreover, all GPMAGs represent the highest MAG qualities (complete and near complete) also belong to Pseudomonadota, underscoring a strong association between MAG quality and prevalence.

Together, these results highlight high-quality and comprehensive assembly of HiFi-based GPMAGs representing valuable genomic resources for the grapevine phyllospheric microbiome investigation.

Annotation of grapevine MAGs reveals genes encoding key biological processes

To delve deeply into functional roles of the GPMAGs in the grapevine microbiome, particularly those derived from unculturable microorganisms, we performed genomic annotation for the GPMAGs using Prokka [36] pipeline. This analysis identified a total of 82,884 genes, comprising 81,801 CDSs, 956 tRNA genes, 96 rRNA genes, 15 tmRNA genes, and 16 repeat regions (**Fig. 4a and Table S5**). Functional annotation of the CDSs was further conducted using eggNOG-mapper v2 [37], and annotated the detailed functions of the CDSs, which identified 67,012 CDSs with various biological process terms. In terms of biological function, proteins with unknown function (26.7%) represented the largest category among the CDSs, and the remaining was primarily associated with core biological functions, such as transcription, metabolism, and transport (**Fig. 4b**). Notably, the top 20 most abundant functional terms accounted for 93.9% of total terms, demonstrating highly focused functional diversity in the GPMAGs that suggests specialized adaptation to the grape phyllosphere niche. Despite biosynthesis of secondary metabolites and microbial metabolism in diverse environments being the predominant biological pathway terms, the top 20 terms represented only 47.9% of total annotations (**Fig. 4c**), demonstrating functional versatility in the GPMAGs. These results indicate both functional consistency and expansive metabolic potentials in the GPMAGs, likely facilitating phyllosphere colonization and adaptation in grapevines.

Agriculture such as viticulture heavily relies on pesticide application in disease

management regime, but their misuse may have inadvertently contributed to the emergence of antimicrobial resistance (AMR) in the crop microbiome [38], posing significant threats to both food safety and public health. Notably, the annotated CDSs from GPMAGs frequently encode proteins associated with antibiotic resistance, such as ABC transporter (**Fig. 4c**), indicating the widespread presence of AMR genes within the GPMAGs. Specifically, we employed RGI [39] to identify 93 AMR genes spanning 16 distinct AMR families, with *adeF* being the most abundant AMR gene conferring resistance to tetracycline and fluoroquinolone (**Fig. 4a, d, S2 and Table S6**). Notably, a significant proportion of the AMR genes exhibited multi-drug resistance through antibiotic efflux, a predominant resistance mechanism. The abundant presence of AMR genes in the grapevine microbiome implies that antibiotic resistance may have occurred due to prolonged pesticide application and misuse in viticulture.

Plant-associated bacterial endophytes protect their plant hosts from external pathogens by producing secondary metabolites (SMs), including antibiotics and toxins [40–42], establishing them as valuable resources for environmentally friendly and pathogen-effective biocontrol agents. Biosynthetic gene clusters (BGCs) responsible for bacterial SM production typically comprise dozens of related genes distributed across extensive genomic regions, necessitating high-quality MAGs with exceptional completeness and continuity for comprehensive exploration. To leverage our high-quality GPMAGs, we employed antiSMASH [43] to identify a total of 96 BGCs from 26 distinct BGC types in the grapevine phyllospheric microbiome (**Fig. 4a, d, S3 and Table S7**). Among these, terpene, RIPP-like, NRPS clusters were the most abundant, commonly associated with antimicrobial activity

critical for host defense [44–46]. Other predominant BGCs, including Ni-siderophore, betalactone, and T3PKS highlight the microbiome's ample potentials in SM productions. These candidate BGCs provide valuable resources for discovering novel natural products and elucidating their roles in grapevine biology and medicinal applications.

Several studies have demonstrated that microorganism-derived polysaccharides play crucial roles in plant bioprocesses, including immune responses, growth facilitation, stress adaptation, photosynthesis, and plant-bacteria interactions [47–49]. To explore the potential of polysaccharides production in the grapevine microbiome, we employed dbCAN [50] to annotate CAZyme genes from the GPMAGs. The analysis identified a total of 1,144 CAZyme genes spanning 143 unique enzyme families, reflecting the grape phyllospheric microbiome's substantial capacity for polysaccharides metabolism (**Fig. 4a, d, S4 and Table S8**). Among these genes, glycosyltransferases (GTs) and glycoside hydrolases (GHs) were particularly abundant, with GT2, GT4, GT51, and GH13 emerging as the most prevalent, suggesting a strong focus on polysaccharide synthesis and modification. Additionally, the presence of diverse carbohydrate-binding modules (CBMs) and auxiliary activities (AAs) highlights the microbiome's versatility and its potential involvement in plant-microbe interactions. This extensive CAZyme repertoire indicates that the grape phyllospheric microbiome may influence various host physiological processes, including disease resistance and growth, through polysaccharide synthesis and other host-interactive mechanisms.

To evaluate the functional potentials of each phylum in terms of antibiotic resistance, secondary metabolite biosynthesis, and carbohydrate metabolism that differentially

influence host biology, we quantified the mean numbers of AMR genes, BGCs, and CAZyme genes of each phylum in the GPMAGs. As a result, Pseudomonadota contained the highest abundance of AMR genes (**Fig. 4e**), indicating particularly strong antibiotic resistance potential. Actinomycetota showed the greatest capacity for secondary metabolite biosynthesis, harboring the most BGCs. While all phyla maintained comparable CAZyme gene numbers, Pseudomonadota demonstrated particularly extensive carbohydrate metabolic potential. These results reveal phylum-specific functional potentials that differentially involve host biological processes.

In conclusion, these findings provide valuable insights into the functional potential of the grapevine phyllospheric microbiome, emphasizing its involvement in shaping host health and resilience through microbial-host interactions.

Downy mildew resistance relates to complexity of microbial interaction network with presence of key genera

To investigate the role of grapevine microbiome during *P. viticola* infection, we profiled the microbiome composition of the grapevine accessions based on their DM disease phenotypes (susceptible or resistant). Unexpectedly, the microbiome compositions of the susceptible and resistant microbiomes were nearly identical (**Fig. S5a**). Additionally, β-diversity analysis further revealed no overall compositional difference between the two groups (**Fig. S5b**), suggesting that microbiome composition unlikely accounts for the differences in DM resistance. Therefore, we hypothesized that interactions within the microbial community

might contribute to the observed resistance. To test this hypothesis, we analyzed the complexity of the microbial interaction networks in the susceptible and resistant grape microbiome using Sparse Inverse Covariance estimation for Ecological Association and Statistical Inference (SpiecEasi) [51] analysis. SpiecEasi uses sparse inverse covariance estimation to identify true associations between microorganisms based on correlations derived from the covariance of their relative abundances. Positive correlations indicate cooperative interactions, while negative correlations represent antagonistic interactions. Remarkably, the resistant microbiome exhibited a significantly more complex network than the susceptible ones (**Fig. 5a**), with a higher frequency of negative interactions per genus (**Fig. S6**), indicating the involvement of microbial network complexity in modulating DM-resistance, especially the negative interactions play crucial role for the complexity.

Notably, the resistant microbiome was highly compartmentalized and centralized around a few genera (e.g., *Lactiplantibacillus*, *Liberibacter, Paracidovorax*, and *Xanthomonas*), with relatively much higher abundance (**Fig. 5a**), suggesting the presence of key genera with pivotal roles in network dynamics and resistance modulation. To identify these key genera, we first profiled the top 100 most abundant genera in the resistant microbiome based on relative abundance and microbial interaction metrics. These profiles were then systematically compared with those from the susceptible microbiome to evaluate their respective contributions to the network complexity. Among them, *Liberibacter* and *Pseudomonas* emerged as the most influential genera, with significantly increased interaction metrics compared to those of the susceptible microbiome (**Fig. 5b**). Intriguingly, all these key genera belong to the core microbiome (**Table S3**), highlighting the importance

of the core microbiome in modulating the complexity. Additionally, genera such as *Bacillus* exhibit increased abundance and interaction metrics compared to the susceptible microbiome, indicating contribution to the complexity via abundance and microbial interaction. Despite relatively low abundances in the resistant microbiome, genera such as Bacteroides, Agathobacter, Bifidobacterium, Anaerobutyricum, and Neisseria exhibit the highest interactions (8-10 interactions/genus) in the resistant microbiome, demonstrating the important role of low abundant genera in forming the complexity. To evaluate phylum-level contributions to the increased complexity, we compared the proportions of microbial interaction between the resistant and susceptible microbiomes for each phylum. As a result, Bacillota was identified as the primary contributors exhibiting the most significantly increased proportion in the resistant microbiome (33.5%) compared to that of the susceptible one (23.9%), while other phyla show minimal fluctuation in the change (**Fig. S7**). Furthermore, we analyzed Spearman correlations between Bacillota and other major phyla in the resistant microbiomes based on their abundances, identifying those with the strongest interactions with this key phylum. The correlation analysis revealed that Euglenozoa, one of the major eukaryotes in the grapevine microbiome (**Fig. 2c**) and Cyanobacteriota exhibits the strongest positive interaction with Bacillota, while the other phyla display no significant positive interactive dynamics (**Fig. S8**), indicating that Bacillota positively interacts with these phyla in the resistant microbiome. These findings suggest that not all genera contribute equally to the modulation of the network complexity; rather, specific key genera play a primary role along with specific interactions.

To validate the effectiveness of key genera profiling and role of key genera during *P.*

viticola infection, we screened microorganisms isolated from the grapevine leaves. Among the key genera, we successfully identified two *Bacillus* strains which belong to Bacillota, *B. cereus* 117 gite and *B. cereus* SW9SE. Given our observation that *Bacillus* is a key genus belong to Bacillota with increased proportion and microbial interactions in the resistant microbiome (**Fig. 5b**), and considering prior reports on *B. cereus* efficacy against grape ripe rot disease [52], we hypothesized and tested the biocontrol potential of *B. cereus* against *P. viticola* infection. To this end, we inoculated grapevine leaf discs with varying concentrations of these strains followed by *P. viticola* infection. Strikingly, both strains exhibited apparent DM inhibition at a low concentration (e.g., OD=0.02) (**Fig. 5c and d**), demonstrating the potent biocontrol activity of the strains against *P. viticola* infection. These findings underscore the effectiveness of our key genera profiling, and paving a way for *B. cereus* as a novel biocontrol resource for managing DM infection in viticulture.

Collectively, our pan-metagenomic analysis and experiments highlight the complexity of the microbial network in mediating DM-resistance, driven by intricate interactions involving specific key genera with specific interactions.

Downy mildew triggers eukaryotic primary and secondary metabolism of the grapevine microbiome

Given that network complexity is primarily driven by Bacillota, which exhibits the strong positive abundance correlation with one of the dominating Eukaryotes-Euglenozoa, we hypothesize that key bacterial phyla involve eukaryotic transcriptomes in the grapevine

microbiome, potentially underlying defensive responses against *P. viticola* infection. To examine this, we conducted pan-metatranscriptomic sequencing and analysis to investigate the transcriptional regulation of the grapevine phyllospheric microbiome in response to the infection. In brief, we collected samples from both infected (one day post-inoculation) and uninfected leaves from 103 of the grapevine accessions and subjected them to RNA-seq [23] (**Fig. 1d**). The RNA-seq reads were mapped to the grapevine and *P. viticola* reference genomes (NCBI accession: GCA_001695595.3), obtaining the unmapped reads that represent eukaryotic organisms other than grapevine and *P. viticola* (**Table S2**). The unmapped reads were then de novo assembled using Trinity [53], resulting in 192,675 eukaryotic transcripts. Differentially expressed transcript (DET) analysis identified 40,546 significantly up-regulated and 5,081 down-regulated transcripts (**Fig. 6a**), indicating a considerable overall upregulation of the microbial transcripts upon the infection. Moreover, KEGG and GO enrichment revealed that the up-regulated genes were primarily involved in primary and secondary metabolisms (**Fig. 6b and c**), with secondary metabolism being particularly prominent in the microbiome's response to the infection. Consistently, Gene Set Enrichment Analysis (GSEA) further confirmed significant enrichment of secondary metabolism-related gene sets among the upregulated transcripts (**Fig. 6d**). Notably, these upregulated transcripts encoded the key proteins of BGCs, including ketoacyl reductase (KR) domains and flavin mononucleotide-dependent dehydrogenases, both of which are integral to the biosynthesis of polyketides and antibiotics [54,55]. Together, these findings demonstrate that primary and secondary metabolisms in eukaryotic microorganisms is significantly induced during *P. viticola* infection, suggesting a potential role for the

grapevine phyllospheric microbiome in defending against pathogen invasion through the competitive exclusion and SM productions that mediated by key bacterial genera.

Discussion

Microbiome have profound impact on physiology and immunity of host organisms ranging from human, animals and plants. Mounting evidence underscores the critical roles of the microbiome in the health, yield, and quality [4,9–11] of grapevine which is one of the most economically important fruit crops cultivated worldwide for production of fresh fruits, wine, juice and raisin etc. Despite a huge body of knowledge gained in microbiome research, pan-microbiome diversity across a genus of host organisms is poorly understood, lacking a large-scale pan-metagenomic approach, especially from long-read sequencing. In this study, combining short- and long-read sequencing, we conducted a pan-metagenomic and pan-metatranscriptomic study of 107 accessions from 34 *Vitis* species to understand the structure, diversity and functional roles of pan-microbiome in grapevine phyllosphere, a key battleground for host-microbe interactions. We identified the core microbiome dominated by Bacillota and Pseudomonadota. Leveraging PacBio HiFi sequencing of grapevine phyllosphere, we successfully assembled 19 high-quality GPMAGs including four near-complete MAGs, with detailed functional annotations, representing the first assembly of MAGs derived from plant HiFi datasets. Furthermore, pan-metagenomic and pan-metatranscriptomic analyses elucidated the underlying defense mechanisms of grape microbiome against *P. viticola* infection. Our findings demonstrate the profound influence

of the microbiome on grapevine biology, particularly involvement in the resistance of *P. viticola* infection, and provide a foundation and valuable genomic and microbial resources for developing microbiome-based biocontrol strategies in viticulture.

Structural analysis of the grapevine phyllosphere microbiome revealed the core microbiome dominated by specific phyla, primarily Bacillota and Pseudomonadota, which constitute the dominant proportion of the microbial community (**Fig. 2**). This composition aligns well with previous studies on grapevine phyllosphere microbiota across different cultivars and geographic regions [4,56–58], highlighting the prevalence and pivotal roles of the core microbiome. However, the mechanisms underlying core microbiome recruitment in the grapevine phyllosphere remain largely unknown. In plants, it is well established that metabolic secretions, particularly SMs such as flavonoids, salicylic acid, and strigolactones, shape microbiome composition through plant-microorganism interactions [59–62]. In turn, the modulated microbiome significantly influences host biological processes via plant-microbe interaction, including growth, disease resistance, and stress responses [59–62]. As a major plant part interacting with microbial communities, common SMs might accumulate in grapevine leaves of diverse genetic background, thereby helping establish the core microbiome. This core microbiome plays critical roles in growth, disease resistance, and stress responses, underscoring the importance of grapevine-microbe interactions in maintaining normal plant development.

Compared to amplicon sequencing analysis, MAGs provide novel and pivotal insights into plant microbiome. Our GPMAGs demonstrate the high quality and prevalence, serving as ideal genomic resources with detailed annotations such as AMR, BGC, and CAZyme

information for further applications. To our knowledge, this is the first study to generate MAGs from HiFi reads of a large collection of plant accessions. However, the rare presence of dominant phyla such as Bacillota in the GPMAGs (**Fig. 3d and Table S4**) highlights the limitations of long-read technology in the number of microbial genomes recovered from microbiome, primarily due to higher cost of sequencing and thus lower data coverage compared to NGS data, and limitation of bioinformatic methods [63,64]. Decreasing sequencing cost and further optimization and advancement of these methods will improve HiFi-based MAG assemblies in the future. Together, this study establishes a novel and robust method for assembling MAGs from plants, leveraging the contiguity and accuracy of HiFi reads to accelerate research on plant microbiome.

It is widely recognized that through interactions microorganisms, plants modulate their immunity to combat pathogen invasion [65,66]. This mechanism primarily relies on microbiome-derived SM production and competitive exclusion to protect host plants from various pathogens. Consistent with this concept, our findings demonstrate the pivotal roles of bacteriome and eukaryome, of which bacteriome re-orchestrates microbial community, especially facilitates interaction with eukaryome to mediate their SM production and competitive exclusion in response to *P. viticola* infection (**Fig. 7**). Intriguingly, we observed a significant increase in network complexity, driven by the contributions of key genera from bacteriome (**Fig. 5 and Fig. S6, 7**), which involves the defense mechanism against *P. viticola* infection in grapevines through interacting with eukaryome. In olive, *Pseudomonas simiae* PICF7, a biological control agent for Verticillium wilt, was reported to significantly increase microbial network complexity upon the infection, resulting in a more stable

network that plays a crucial role in defense [67]. Thus, it is likely that grapevines employ a similar strategy to modulate their microbial network, optimizing SM production and competitive exclusion capacities of eukaryome to effectively combat *P. viticola* infection. Additionally, the profiling of key genera in the DM-resistant microbiome provides a valuable resource for exploring biocontrol microorganisms against *P. viticola* infection exemplified by the experimental validation of two *B. cereus* strains, laying the foundation for environmentally friendly and sustainable biocontrol strategies in viticulture.

Materials and methods

Collection of grapevine leaves for metagenome sequencing

The leaf samples from 107 grapevine accessions used in this study were collected from vineyards at the Zhengzhou Fruit Research Institute, Chinese Academy of Sciences (Zhengzhou, Henan, China), and the Institute of Advanced Agricultural Sciences, Peking University (Weifang, Shandong, China). All grapevines were maintained under standard management practices, including regular cultivation, watering, fertilization, pruning, and disease control.

Downy mildew infection assay

DM infection was performed as described previously [68]. Each grapevine leaf disc (8 mm in diameter) was inoculated with 20 μL of *P. viticola* suspension (1×10^5 sporangia/mL) on the abaxial surface and incubated at 18 ± 2°C with 80 ± 10% relative humidity in a growth

chamber under a 12 h light (60 μmol·m^{-2}·s^{-1})/12 h dark cycle. Leaf discs were collected 24 hours post-inoculation for transcriptome analysis. At least three biological replicates were conducted, with each replicate comprising five leaf discs from different grapevines.

DNA and RNA extraction

Genomic DNA for NGS was extracted from the grapevine leaves using DNeasy Plant Mini Kit (QIAGEN, Hilden, Germany) according to the manufacturer's instructions. The DNA integrity was assessed with an Agilent 4200 Bioanalyzer (Agilent Technologies, Santa Clara, USA). High-molecular-weight (HMW) DNA for HiFi sequencing was prepared from the fresh grapevine leaves using the cetyltrimethylammonium bromide (CTAB) method [69]. The DNA quality was verified with 1% agarose gel electrophoresis, and purity was assessed using a NanoPhotometer® spectrophotometer (IMPLEN, Westlake Village, USA). The DNA concentration was measured with a Qubit® 2.0 Fluorometer (Life Technologies, Carlsbad, USA). Total RNA was extracted using TRIzol reagent (Thermo Fisher Scientific, Waltham, USA) following the manufacturer's instructions. The RNA concentration was measured with a Nanodrop 2000 spectrophotometer (Thermo Fisher Scientific, Waltham, USA), and the purity was evaluated using a NanoPhotometer® (IMPLEN, Westlake Village, USA). The RNA concentration and integrity were further analyzed with an Agilent 2100 Bioanalyzer using the RNA Nano 6000 assay kit (Agilent Technologies, Santa Clara, USA).

Metagenome sequencing

For NGS library preparation, 15 μg of the genomic DNA was sheared using g-Tubes (Covaris, Woburn, USA) and concentrated with AMPure PB magnetic beads (Pacific Biosciences, Menlo Park, USA). The library construction was performed with 1 μg of the DNA template following TruSeq DNA Sample Preparation Guide (Illumina, San Diego, USA). Paired-end sequencing was conducted on a HiSeq X Ten platform (Biomarker Technologies, Qingdao, China), generating 150 bp NGS reads. For HiFi sequencing, 15 μg of the purified HMW genomic DNA was used to construct a standard SMRTbell library with SMRT Express Template Prep Kit 2.0 (Pacific Biosciences, Menlo Park, USA). Circular consensus sequencing (CCS) producing HiFi reads was performed on a PacBio Sequel IIe system at Biomarker Technologies (Qingdao, China). To prepare RNA sequencing libraries, 1-3 μg of the total RNA was used as input for library construction with VAHTS Universal V6 RNA-seq Library Prep Kit for Illumina® (Vazyme, Nanjing, China) according to the manufacturer's instructions. The RNA concentration was initially quantified with the Qubit® RNA Assay Kit on a Qubit® 3.0 (Thermo Fisher Scientific, Waltham, USA) and diluted to 1 ng/μl. Insert size was measured with an Agilent Bioanalyzer 2100 (Agilent Technologies, Santa Clara, USA), and final library concentration (>10 nM) was verified with a Bio-RAD CFX 96 quantitative PCR system (Bio-Rad, Hercules, USA). Paired-end sequencing was then performed on a HiSeq X Ten platform (Biomarker Technologies, Qingdao, China), generating 150 bp RNA-seq reads.

Quality control and removal of host reads

To ensure the quality of the short reads, quality control was performed on the NGS and RNA-seq reads using fastp [70] (v0.23.4) with default parameters, resulting in the quality-controlled reads. To completely filter out reads from the grapevine hosts, the NGS, HiFi, and RNA-seq reads were mapped to the complete reference genome of *Vitis vinifera* [23] (VHP-T2T.hap1, NCBI accession: GCA_046255155.1) using Minimap2 [71] (v2.28) with parameters (NGS, RNA-seq:-ax sr, HiFi:-ax map-pb). The mapped results were further filtered using SAMtools [72] (v1.21) with parameters (NGS, RNA-seq: view -u -f 12 -F 256, HiFi: view -f 4 -F 256) to retain microbial reads. Additionally, the RNA-seq reads were further filtered by mapping to *P. viticola* reference genome INRA_Pvit_2 (NCBI accession: GCA_001695595.3) with Minimap2 and SAMtools to exclude *P. viticola* reads.

Taxonomic classification

To profile the taxonomic composition of the grapevine microbiome, the filtered NGS reads were taxonomically classified using Kraken2 [24] (v2.1.3) and k2_pluspf_20240904 database with parameters (--paired --confidence 0.1 --minimum-hit-groups 2), yielding the compositional statistics of the grapevine microbiome.

Pan-metagenomic and diversity analysis

The identification of the core, dispensable, and unique microbiome was conducted with R using the microbial composition statistics. To assess microbiome diversity, PCoA analysis was performed with vegan [73] (v2.6-8) package in R. All statistical analysis and

visualization were performed with R.

Assembly of the GPMAGs

To generate the GPMAGs, the filtered HiFi reads were assembled using Flye [26] (v2.9.5), Hifiasm [27] (v0.19.9), Hifiasm-meta [28] (vhamtv0.3.2), metaFlye [29] (v2.9.5), MetaMDBG [30] (v1.0), and Verkko [31] (v2.2.1) with default parameters to produce initial contig assemblies. The resulting contigs were then binned with CONCOCT [32] (v1.1.0), MaxBin2 [33] (v2.2.7), and MetaBAT2 [34] (v 2.17) with default parameters. The bins were quality-checked using CheckM2 [74] (v1.0.2), and those meeting the medium-quality criterion [30] were dereplicated to generate non-redundant GPMAGs using Galah (v0.4.2) (https://github.com/wwood/galah) with parameters (--ani 95 --precluster-ani 90 --min-aligned-fraction 30 --min-completeness 50 --max-contamination 10).

Taxonomic and phylogenetic analysis of the GPMAGs

To reveal the taxonomic composition of the GPMAGs, GTDB-Tk [35] (v2.4.0) was employed with the R220 database and default parameters, generating the taxonomic composition and a multiple sequence alignment (MSA) file. The MSA file was further subjected to the construction of phylogenetic tree using IQ-TREE2 [75] (v2.1.4_beta) with default parameters, and visualized by iTOL [76] (https://itol.embl.de/).

Functional annotation of the GPMAGs

To analyze different gene types from the GPMAGs, Prokka [36] (v1.14.6) was used for gene type prediction with default parameters. The predicted CDSs were further applied for functional annotation using eggNOG-mapper [77] (2.1.12) with parameters (-m diamond --evalue 1e-5 --query_cover 50 --subject_cover 50). To annotate AMR genes, BGCs, and CAZyme genes of the GPMAGs, RGI [39] (v6.0.3) (default parameters), antiSMASH [43] (v7.1.0) (parameters: --genefinding-tool prodigal --taxon bacteria –fullhmmer --cb-knownclusters --cb-subclusters --cc-mibig --asf --rre --pfam2go), and dbCAN [50] (v4.1.4) (default parameters) were employed, respectively.

Construction of microbial interaction network

Microbial interaction network was constructed using the microbial composition statistics and SpiecEasi [51] (v1.1.3) package in R with parameters (lambda.min.ratio=0.5, nlambda=30, rep.num=100).

Isolation of grapevine phyllosphere microorganisms

To isolate microorganisms from grapevine leaves, we collected leaves from *V. vinifera* cv. Chardonnay, *V. vinifera* cv. Muscat Hamburg, *V. vinifera* x *V. labrusca* cv. Kyoho, and *V. vinifera* x *V. labrusca* cv. Vidal Blanc at the vineyards. After rinsing with sterile water, the leaves were homogenized in 1x PBS buffer using an electric mixer to obtain a microbial

suspension. 2 ml of the suspension were inoculated onto Nutrient Agar medium (Coolaber Technology Co., Ltd., Beijing, China) and incubated at 30°C for 24 hours. Single colonies were isolated and further purified by streaking on Nutrient Agar medium. Species identification was performed by 16S rRNA sequencing (Tsingke Biotechnology Co., Ltd., Beijing, China).

Experimental validation of biocontrol activity

To validate the efficacy of isolated microorganisms against *P. viticola* infection, the *B. cereus* strains were cultured in Nutrient Broth medium (Coolaber Technology Co., Ltd., Beijing, China) at 30°C and 220 rpm for 12 hours. The cultures were diluted to OD of 0.02 at 600 nm using a Nanodrop 2000 spectrophotometer (Thermo Fisher Scientific, Waltham, USA). The diluted suspensions were sprayed onto 1 cm grape leaf discs and incubated at 30°C and 220 rpm for 24 hours. Subsequently, *P. viticola* was co-inoculated onto the discs using the method described above and incubated at 19°C for 6 days. Disease severity was assessed 6 days post-inoculation using the following grading scale: Grade 0, no lesions (0% of leaf disc area affected); Grade 1, lesions covering less than 10% of the leaf disc area; Grade 2, lesions covering 10-30% of the leaf disc area; Grade 3, lesions covering 31-60% of the leaf disc area; Grade 4, lesions covering 61-80% of the leaf disc area; and Grade 5, lesions covering more than 80% of the leaf disc area. The disease index (DI) was calculated as follows:

$$DI = \frac{\sum(s_i\, n_{i2})}{N_2 5}\, 100$$

where s_i represents the disease grade (ranging from 0 to 5), n_{i2} is the number of leaf discs with disease grade s_i , and N_2 is the total number of leaf discs assessed. The DI value was rounded to one decimal place.

Transcriptomic analysis of *P. viticola* infection

Transcriptomic profiling in response to *P. viticola* infection was conducted using the filtered RNA-seq reads. First, *De novo* assembly of transcripts was performed with Trinity [53] (v2.15.2) using default parameters. The generated transcripts were dereplicated using VSEARCH [78] (2.29.0) with parameters (--id 0.95), selecting the longest transcripts as the representatives of duplicates. Transcript expression was quantified using Salmon [79] (v1.10.3) with default parameters and the filtered RNA-seq reads. Differential expression analysis was performed with the DESeq2 [80] (v1.45) package in R. Subsequently, the significantly up-regulated genes were further annotated with eggNOG-mapper, followed by KEGG, GO, and GSEA enrichment analyses using AnnotationForge (v1.47.1), AnnotationDbi (v1.67.0), ClusterProfiler [81] (v4.13.3) and enrichplot (v1.25.2) packages in R with default parameters.

Acknowledgments

We would like to thank the Bioinformatics Platform at Peking University Institute of Advanced Agricultural Sciences for providing the high-performance computing resources.

Author contributions

LG and WXY conceived and supervised the study. JYJ, XNZ, JJM, WZ, LLG, HSS, CHL and LLZ prepared the plant samples and performed the experiments. JYJ and XFW conducted the bioinformatics analysis. JYJ, LG and WXY wrote and revised the manuscript. All authors read and approved the final manuscript.

Funding

This project was supported by Key R&D Program of Shandong Province (Grant No. 2024CXPT031 and ZR202211070163) and the Taishan Scholars Program of Shandong Province. LG is also supported by the Natural Science Foundation for Distinguished Young Scholars of Shandong Province (Grant No. ZR2023JQ010). JYJ is supported by the Shandong Provincial Natural Science Foundation Youth Project (Grant No. ZR2024QC241).

Competing interests

The authors declare no competing interests.

References

1. Food and Agriculture Organization of the United Nations. FAOSTAT. Rome; 2024.

2. Zhou DD, Li J, Xiong RG, Saimaiti A, Huang SY, Wu SX, et al. Bioactive Compounds, Health Benefits and Food Applications of Grape. Foods. MDPI; 2022.

3. Buonassisi D, Colombo M, Migliaro D, Dolzani C, Peressotti E, Mizzotti C, et al. Breeding for grapevine downy mildew resistance: a review of "omics" approaches. Euphytica. Springer Netherlands; 2017.

4. Bettenfeld P, Cadena i Canals J, Jacquens L, Fernandez O, Fontaine F, van Schaik E, et al. The microbiota of the grapevine holobiont: A key component of plant health. J Adv Res. Elsevier B.V.; 2022. p. 1–15.

5. Campos G, Chialva C, Miras S, Lijavetzky D. New Technologies and Strategies for Grapevine Breeding Through Genetic Transformation. Front Plant Sci. Frontiers Media S.A.; 2021.

6. Cantu D, Walker MA. Compendium of Plant Genomes The Grape Genome [Internet]. Available from: http://www.springer.com/series/11805

7. Magon G, De Rosa V, Martina M, Falchi R, Acquadro A, Barcaccia G, et al. Boosting grapevine breeding for climate-smart viticulture: from genetic resources to predictive genomics. Front Plant Sci. Frontiers Media SA; 2023.

8. Peng J, Wang X, Wang H, Li X, Zhang Q, Wang M, et al. Advances in understanding grapevine downy mildew: From pathogen infection to disease management. Mol Plant Pathol. John Wiley and Sons Inc; 2024.

9. Bokulich NA, Thorngate JH, Richardson PM, Mills DA. Microbial biogeography of wine grapes is conditioned by cultivar, vintage, and climate. Proceedings of the National Academy of Sciences. 2014;111.

10. Ding Y, Wei R, Wang L, Wang W, Wang H, Li H. Exploring the ecological characteristics of natural microbial communities along the continuum from grape berries to winemaking. Food Research International. 2023;167.

11. Bokulich NA, Collins TS, Masarweh C, Allen G, Heymann H, Ebeler SE, et al. Associations among wine grape microbiome, metabolome, and fermentation behavior suggest microbial contribution to regional wine characteristics. mBio. 2016;7.

12. Awad M, Giannopoulos G, Mylona P V., Polidoros AN. Comparative Analysis of Grapevine Epiphytic Microbiomes among Different Varieties, Tissues, and Developmental Stages in the Same Terroir. Applied Sciences. 2022;13:102.

13. Wei T-L, Zheng Y-P, Wang Z-H, Shang Y-X, Pei M-S, Liu H-N, et al. Comparative microbiome analysis reveals the variation in microbial communities between 'Kyoho' grape and its bud mutant variety. PLoS One. 2023;18:e0290853.

14. Vitulo N, Lemos WJF, Calgaro M, Confalone M, Felis GE, Zapparoli G, et al. Bark and Grape Microbiome of Vitis vinifera: Influence of Geographic Patterns and Agronomic Management on Bacterial Diversity. Front Microbiol. 2019;9.

15. Bao L, Sun B, Wei Y, Xu N, Zhang S, Gu L, et al. Grape Cultivar Features Differentiate the Grape Rhizosphere Microbiota. Plants. 2022;11:1111.

16. Awad M, Giannopoulos G, Mylona P V., Polidoros AN. Genotype May Influence Bacterial Diversity in Bark and Bud of Vitis vinifera Cultivars Grown under the Same Environment. Applied Sciences. 2020;10:8405.

17. Swift JF, Migicovsky Z, Trello GE, Miller AJ. Grapevine bacterial communities display compartment-specific dynamics over space and time within the Central Valley of California.

Environ Microbiome. 2023;18:84.

18. Fernandes P, Afonso IM, Pereira J, Rocha R, Rodrigues AS. Epiphitic Microbiome of Alvarinho Wine Grapes from Different Geographic Regions in Portugal. Biology (Basel). 2023;12:146.

19. Zhang J, Wang ET, Singh RP, Guo C, Shang Y, Chen J, et al. Grape berry surface bacterial microbiome: impact from the varieties and clones in the same vineyard from central China. J Appl Microbiol. 2019;126:204–14.

20. Coller E, Cestaro A, Zanzotti R, Bertoldi D, Pindo M, Larger S, et al. Microbiome of vineyard soils is shaped by geography and management. Microbiome. 2019;7:140.

21. Kim CY, Ma J, Lee I. HiFi metagenomic sequencing enables assembly of accurate and complete genomes from human gut microbiota. Nat Commun. 2022;13.

22. Ding Y, Zhao L, Wang G, Shi Y, Guo G, Liu C, et al. PacBio sequencing of human fecal samples uncovers the DNA methylation landscape of 22 673 gut phages. Nucleic Acids Res. 2023;51:12140–9.

23. Guo L, Wang X, Ayhan DH, Rhaman MS, Yan M, Jiang J, et al. Super pangenome of Vitis empowers identification of downy mildew resistance genes for grapevine improvement. Nat Genet [Internet]. 2025; Available from: https://www.nature.com/articles/s41588-025-02111-7

24. Wood DE, Lu J, Langmead B. Improved metagenomic analysis with Kraken 2. Genome Biol. 2019;20.

25. Liang Z, Duan S, Sheng J, Zhu S, Ni X, Shao J, et al. Whole-genome resequencing of 472 Vitis accessions for grapevine diversity and demographic history analyses. Nat

Commun. 2019;10.

26. Kolmogorov M, Yuan J, Lin Y, Pevzner PA. Assembly of long, error-prone reads using repeat graphs. Nat Biotechnol. 2019;37:540–6.

27. Cheng H, Concepcion GT, Feng X, Zhang H, Li H. Haplotype-resolved de novo assembly using phased assembly graphs with hifiasm. Nat Methods. 2021;18:170–5.

28. Feng X, Cheng H, Portik D, Li H. Metagenome assembly of high-fidelity long reads with hifiasm-meta. Nat Methods. 2022;19:671–4.

29. Kolmogorov M, Bickhart DM, Behsaz B, Gurevich A, Rayko M, Shin SB, et al. metaFlye: scalable long-read metagenome assembly using repeat graphs. Nat Methods. 2020;17:1103–10.

30. Benoit G, Raguideau S, James R, Phillippy AM, Chikhi R, Quince C. High-quality metagenome assembly from long accurate reads with metaMDBG. Nat Biotechnol. 2024;42:1378–83.

31. Rautiainen M, Nurk S, Walenz BP, Logsdon GA, Porubsky D, Rhie A, et al. Telomere-to-telomere assembly of diploid chromosomes with Verkko. Nat Biotechnol. 2023;41:1474–82.

32. Alneberg J, Bjarnason BS, De Bruijn I, Schirmer M, Quick J, Ijaz UZ, et al. Binning metagenomic contigs by coverage and composition. Nat Methods. 2014;11:1144–6.

33. Wu YW, Simmons BA, Singer SW. MaxBin 2.0: An automated binning algorithm to recover genomes from multiple metagenomic datasets. Bioinformatics. 2016;32:605–7.

34. Kang DD, Li F, Kirton E, Thomas A, Egan R, An H, et al. MetaBAT 2: An adaptive binning algorithm for robust and efficient genome reconstruction from metagenome

assemblies. PeerJ. 2019;2019.

35. Chaumeil PA, Mussig AJ, Hugenholtz P, Parks DH. GTDB-Tk: A toolkit to classify genomes with the genome taxonomy database. Bioinformatics. 2020;36:1925–7.

36. Seemann T. Prokka: Rapid prokaryotic genome annotation. Bioinformatics. 2014;30:2068–9.

37. Cantalapiedra CP, Herṇandez-Plaza A, Letunic I, Bork P, Huerta-Cepas J. eggNOG-mapper v2: Functional Annotation, Orthology Assignments, and Domain Prediction at the Metagenomic Scale. Mol Biol Evol. 2021;38:5825–9.

38. Miller SA, Ferreira JP, Lejeune JT. Antimicrobial Use and Resistance in Plant Agriculture: A One Health Perspective. Agriculture (Switzerland). 2022;12.

39. Alcock BP, Huynh W, Chalil R, Smith KW, Raphenya AR, Wlodarski MA, et al. CARD 2023: expanded curation, support for machine learning, and resistome prediction at the Comprehensive Antibiotic Resistance Database. Nucleic Acids Res. 2023;51:D690–9.

40. Singh K, Birinchiikumarrsarmaaeditors S. Emerging Trends in Plant Pathology. 2020.

41. Narayanan Z, Glick BR. Secondary Metabolites Produced by Plant Growth-Promoting Bacterial Endophytes. Microorganisms. MDPI; 2022.

42. Su P, Kang H, Peng Q, Wicaksono WA, Berg G, Liu Z, et al. Microbiome homeostasis on rice leaves is regulated by a precursor molecule of lignin biosynthesis. Nat Commun. 2024;15.

43. Blin K, Shaw S, Augustijn HE, Reitz ZL, Biermann F, Alanjary M, et al. AntiSMASH 7.0: New and improved predictions for detection, regulation, chemical structures and visualisation. Nucleic Acids Res. 2023;51:W46–50.

44. Ranjan A, Rajput VD, Prazdnova EV, Gurnani M, Bhardwaj P, Sharma S, et al. Nature's Antimicrobial Arsenal: Non-Ribosomal Peptides from PGPB for Plant Pathogen Biocontrol. Fermentation. Multidisciplinary Digital Publishing Institute (MDPI); 2023.

45. Ninkuu V, Zhang L, Yan J, Fu Z, Yang T, Zeng H. Biochemistry of terpenes and recent advances in plant protection. Int J Mol Sci. MDPI; 2021.

46. Li Y, Rebuffat S. The manifold roles of microbial ribosomal peptide-based natural products in physiology and ecology. Journal of Biological Chemistry. American Society for Biochemistry and Molecular Biology Inc.; 2020. p. 34–54.

47. Salachna P, Mizielińska M, Soból M. Exopolysaccharide gellan gum and derived oligo-gellan enhance growth and antimicrobial activity in eucomis plants. Polymers (Basel). 2018;10.

48. Castiblanco LF, Sundin GW. New insights on molecular regulation of biofilm formation in plant-associated bacteria. J Integr Plant Biol. 2016;58:362–72.

49. Carezzano ME, Alvarez Strazzi FB, Pérez V, Bogino P, Giordano W. Exopolysaccharides Synthesized by Rhizospheric Bacteria: A Review Focused on Their Roles in Protecting Plants against Stress. Appl Microbiol. Multidisciplinary Digital Publishing Institute (MDPI); 2023. p. 1249–61.

50. Zheng J, Ge Q, Yan Y, Zhang X, Huang L, Yin Y. DbCAN3: Automated carbohydrate-Active enzyme and substrate annotation. Nucleic Acids Res. 2023;51:W115–21.

51. Kurtz ZD, Müller CL, Miraldi ER, Littman DR, Blaser MJ, Bonneau RA. Sparse and Compositionally Robust Inference of Microbial Ecological Networks. PLoS Comput Biol. 2015;11.

52. Aoki T, Aoki Y, Ishiai S, Otoguro M, Suzuki S. Impact of Bacillus cereus NRKT on grape ripe rot disease through resveratrol synthesis in berry skin. Pest Manag Sci. 2017;73:174–80.

53. Grabherr MG, Haas BJ, Yassour M, Levin JZ, Thompson DA, Amit I, et al. Full-length transcriptome assembly from RNA-Seq data without a reference genome. Nat Biotechnol. 2011;29:644–52.

54. Klaus M, Grininger M. Engineering strategies for rational polyketide synthase design. Nat Prod Rep. Royal Society of Chemistry; 2018. p. 1070–81.

55. Valton J, Filisetti L, Fontecave M, Nivière V. A two-component flavin-dependent monooxygenase involved in actinorhodin biosynthesis in Streptomyces coelicolor. ArXiv [Internet]. 2015 [cited 2024 Dec 13]; Available from: https://arxiv.org/abs/1501.01469

56. Cui S, Zhou L, Fang Q, Xiao H, Jin D, Liu Y. Growth period and variety together drive the succession of phyllosphere microbial communities of grapevine. Science of the Total Environment. 2024;950.

57. Singh P, Santoni S, Weber A, This P, Péros JP. Understanding the phyllosphere microbiome assemblage in grape species (Vitaceae) with amplicon sequence data structures. Sci Rep. 2019;9.

58. Singh P, Santoni S, This P, Péros JP. Genotype-environment interaction shapes the microbial assemblage in grapevine's phyllosphere and carposphere: An ngs approach. Microorganisms. 2018;6.

59. Compant S, Cassan F, Kostić T, Johnson L, Brader G, Trognitz F, et al. Harnessing the plant microbiome for sustainable crop production. Nat Rev Microbiol. Nature Research;

2024.

60. Musilova L, Ridl J, Polivkova M, Macek T, Uhlik O. Effects of secondary plant metabolites on microbial populations: Changes in community structure and metabolic activity in contaminated environments. Int J Mol Sci. MDPI AG; 2016.

61. Rodriguez PA, Rothballer M, Chowdhury SP, Nussbaumer T, Gutjahr C, Falter-Braun P. Systems Biology of Plant-Microbiome Interactions. Mol Plant. Cell Press; 2019. p. 804–21.

62. Pang Z, Chen J, Wang T, Gao C, Li Z, Guo L, et al. Linking Plant Secondary Metabolites and Plant Microbiomes: A Review. Front Plant Sci. Frontiers Media S.A.; 2021.

63. Gand M, Bloemen B, Vanneste K, Roosens NHC, De Keersmaecker SCJ. Comparison of 6 DNA extraction methods for isolation of high yield of high molecular weight DNA suitable for shotgun metagenomics Nanopore sequencing to detect bacteria. BMC Genomics. 2023;24.

64. Portik DM, Brown CT, Pierce-Ward NT. Evaluation of taxonomic classification and profiling methods for long-read shotgun metagenomic sequencing datasets. BMC Bioinformatics. 2022;23.

65. Trivedi P, Leach JE, Tringe SG, Sa T, Singh BK. Plant–microbiome interactions: from community assembly to plant health. Nat Rev Microbiol. Nature Research; 2020. p. 607–21.

66. Vannier N, Agler M, Hacquard S. Microbiota-mediated disease resistance in plants. PLoS Pathog. 2019;15.

67. Cardoni M, Fernández-González AJ, Valverde-Corredor A, Fernández-López M, Mercado-Blanco J. Co-occurrence network analysis unveils the actual differential impact

on the olive root microbiota by two Verticillium wilt biocontrol rhizobacteria. Environ Microbiome. 2023;18.

68. Ma T, Chen S, Liu J, Fu P, Wu W, Song S, et al. Plasmopara viticola effector PvRXLR111 stabilizes VvWRKY40 to promote virulence. Mol Plant Pathol. 2021;22:231–42.

69. Porebski S, Bailey LG, Baum BR. Modification of a CTAB DNA Extraction Protocol for Plants Containing High Polysaccharide and Polyphenol Components. Plant Mol Biol Report.

70. Chen S, Zhou Y, Chen Y, Gu J. Fastp: An ultra-fast all-in-one FASTQ preprocessor. Bioinformatics. Oxford University Press; 2018. p. i884–90.

71. Li H. Minimap2: Pairwise alignment for nucleotide sequences. Bioinformatics. 2018;34:3094–100.

72. Li H, Handsaker B, Wysoker A, Fennell T, Ruan J, Homer N, et al. The Sequence Alignment/Map format and SAMtools. Bioinformatics. 2009;25:2078–9.

73. Dixon P. VEGAN, a package of R functions for community ecology. Journal of Vegetation Science. Opulus Press AB; 2003. p. 927–30.

74. Chklovski A, Parks DH, Woodcroft BJ, Tyson GW. CheckM2: a rapid, scalable and accurate tool for assessing microbial genome quality using machine learning. Nat Methods. 2023;20:1203–12.

75. Minh BQ, Schmidt HA, Chernomor O, Schrempf D, Woodhams MD, Von Haeseler A, et al. IQ-TREE 2: New Models and Efficient Methods for Phylogenetic Inference in the Genomic Era. Mol Biol Evol. 2020;37:1530–4.

76. Letunic I, Bork P. Interactive Tree of Life (iTOL) v6: Recent updates to the phylogenetic

tree display and annotation tool. Nucleic Acids Res. 2024;52:W78–82.

77. Cantalapiedra CP, Herņandez-Plaza A, Letunic I, Bork P, Huerta-Cepas J. eggNOG-mapper v2: Functional Annotation, Orthology Assignments, and Domain Prediction at the Metagenomic Scale. Mol Biol Evol. 2021;38:5825–9.

78. Rognes T, Flouri T, Nichols B, Quince C, Mahé F. VSEARCH: A versatile open source tool for metagenomics. PeerJ. 2016;2016.

79. Patro R, Duggal G, Love MI, Irizarry RA, Kingsford C. Salmon provides fast and bias-aware quantification of transcript expression. Nat Methods. 2017;14:417–9.

80. Love MI, Huber W, Anders S. Moderated estimation of fold change and dispersion for RNA-seq data with DESeq2. Genome Biol. 2014;15.

81. Yu G, Wang LG, Han Y, He QY. ClusterProfiler: An R package for comparing biological themes among gene clusters. OMICS. 2012;16:284–7.

Figures

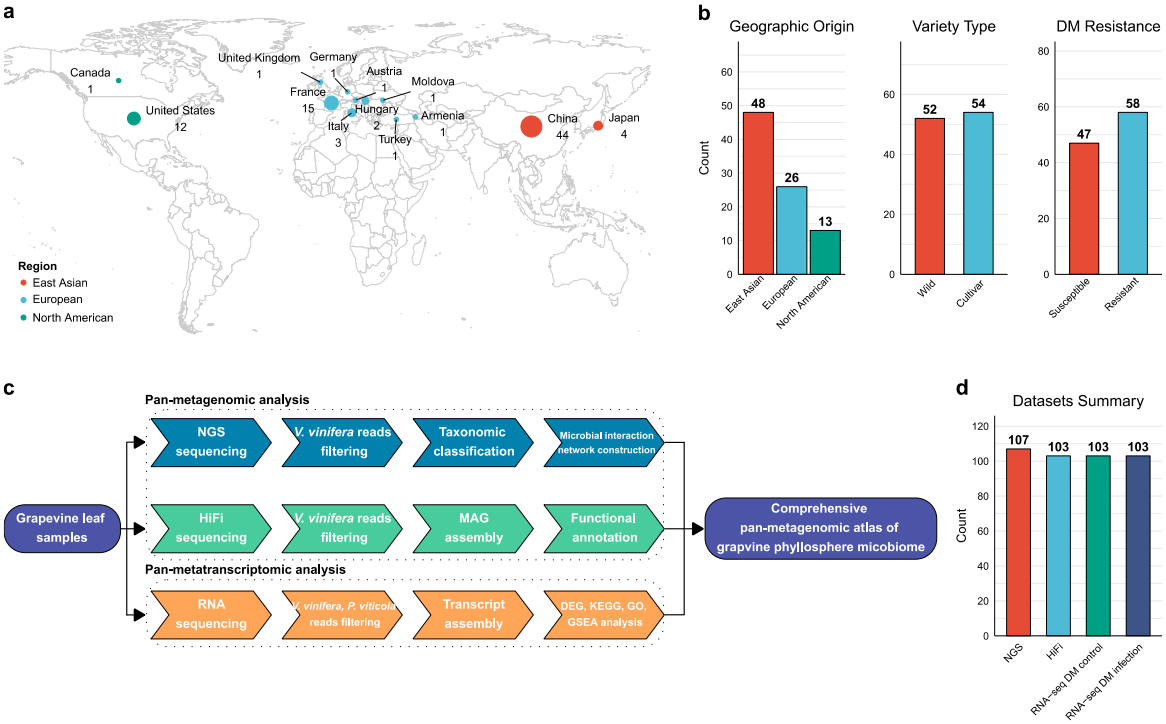

Fig. 1 Research design for grapevine phyllosphere pan-metagenomics and pan-metatranscriptomics. a, Geographical origins of the sampled grapevine accessions. Numbers of samples were numerically labeled. **b**, Classification statistics of grapevine accessions by geographical origin, cultivar type, and DM resistance status. **c**, Pan-metagenomic and pan-metatranscriptomic analysis workflow. Colored blocks indicate sequencing methods: blue (NGS), green (HiFi), orange (RNA-seq), and purple (shared components). **d**, Summary of generated datasets.

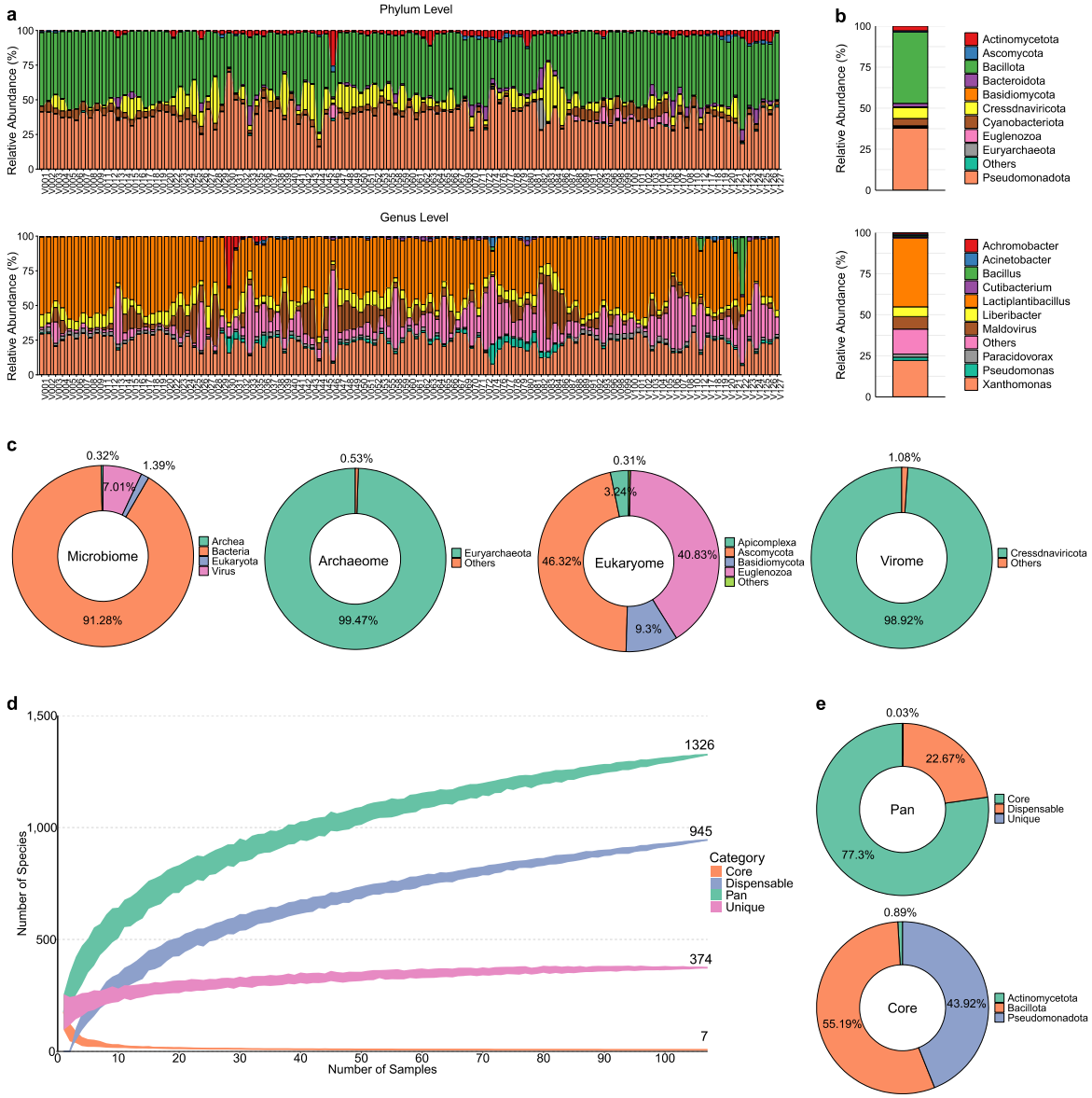

Fig. 2 Pan-metagenomic landscape of the grapevine phyllospheric microbiome. a, Relative abundances of the 10 most abundant phyla (top) and genera (bottom) across the grapevine accessions. **b**, Mean relative abundance of the phyla and genera shown in (**a**). **c**, Compositional profiles of kingdoms from the grapevine accessions. **d**, Pan-metagenomic accumulation curve demonstrating pan, core, dispensable and unique genera across the grapevine accessions. **e**, Pan-metagenomic relative abundance at the genus level within the entire pan-metagenome (top) and the top 10 most abundant phyla within the core microbiome (bottom).

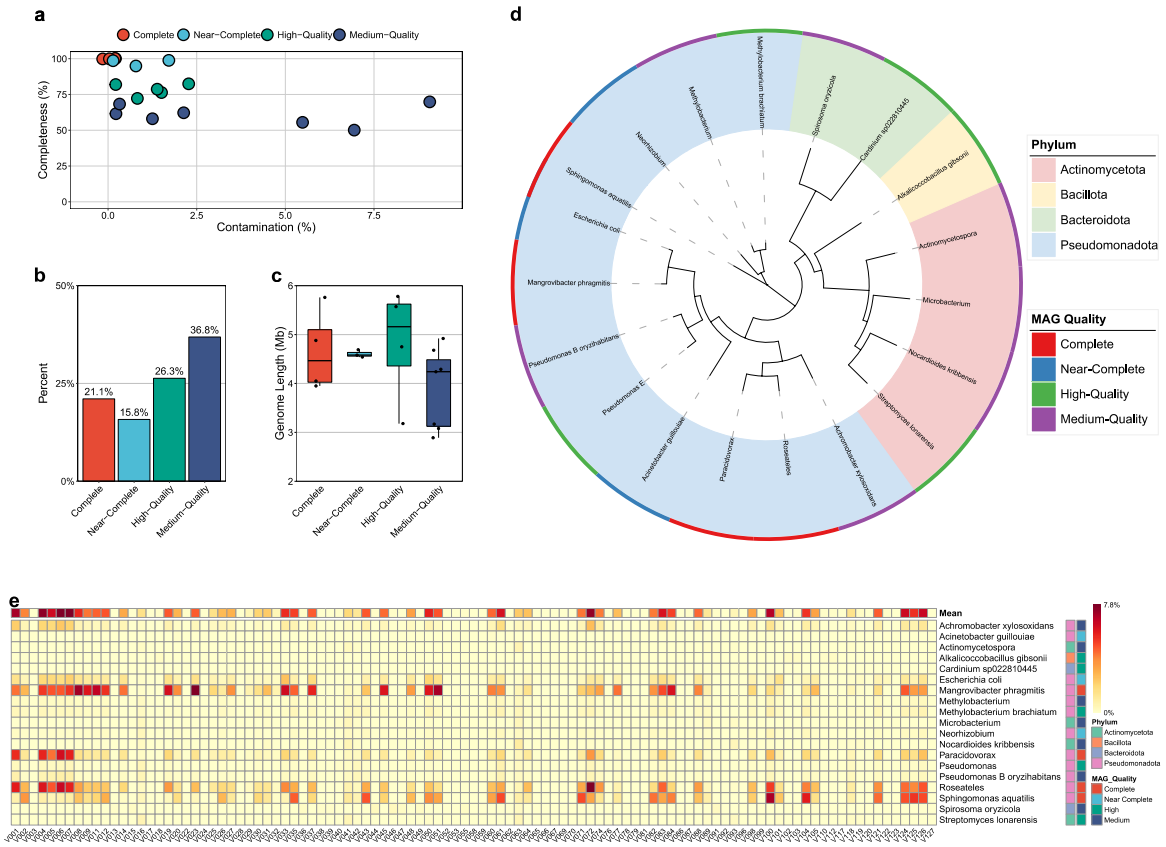

Fig. 3 Assembly and genomic profile of the grapevine phyllospheric metagenome-assembled genomes (GPMAGs). **a**, Quality distribution of the GPMAGs in terms of MAG completeness and contamination. **b**, Composition of the GPMAG quality categories. **c**, Genomic size distribution of the GPMAGs. **d**, Phylogenetic tree of the classified GPMAGs, illustrating corresponding phyla and MAG qualities. **e**, Pan-genomic prevalence of the GPMAGs across the grapevine accessions. Heatmap depicts the relative abundance of the GPMAGs relative to each grapevine HiFi data accession.

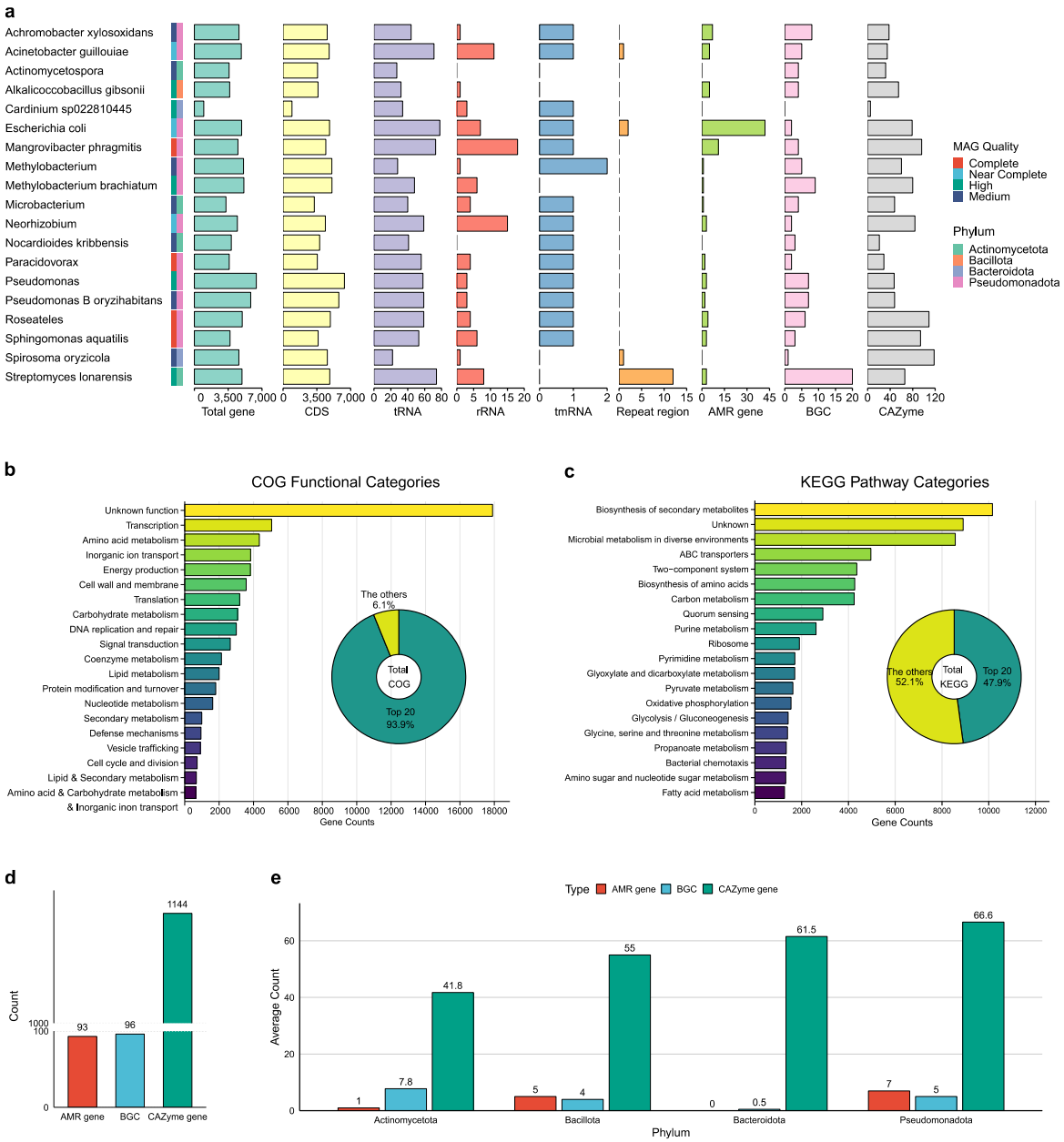

Fig. 4 Functional annotation of the GPMAGs. **a**, Gene type distributions in the GPMAGs. **b-c**, Top 20 COG (**b**) and KEGG pathway (**c**) profiles of the GPMAGs. Donut plots displaying proportions of top 20 terms within total terms. **d**, Statistical summary of AMR, BGC, and CAZyme-associated genes. **e**, Phylum-level functional capacity displayed as mean AMR/BGC/CAZyme-associated gene counts per phylum.

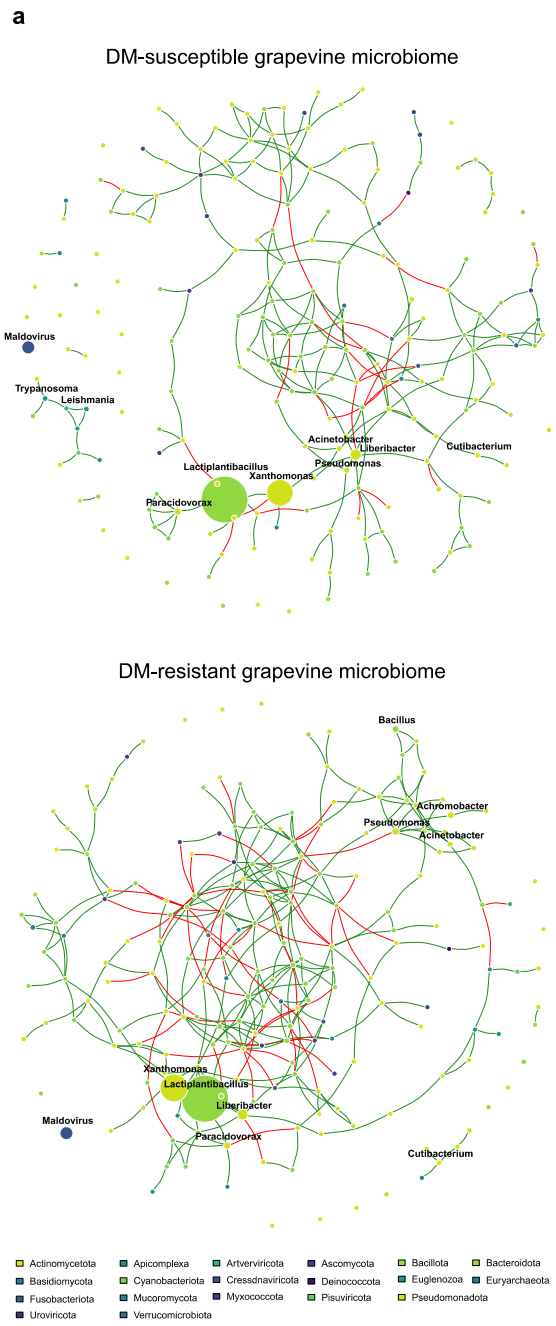
a
DM-susceptible grapevine microbiome
Maldovirus
Trypanosoma
Leishmania
Acinetobacter
Liberibacter
Cutibacterium
Lactiplantibacillus
Pseudomonas
Xanthomonas
Paracidovorax
DM-resistant grapevine microbiome
Bacillus
Achromobacter
Pseudomonas
Acinetobacter
Xanthomonas
Lactiplantibacillus
Liberibacter
Maldovirus
Paracidovorax
Cutibacterium
Actinomycetota
Basidiomycota
Fusobacteriota
Uroviricota
Apicomplexa
Cyanobacteriota
Mucoromycota
Verrucomicrobiota
Artverviricota
Cressdnaviricota
Myxococcota
Ascomycota
Deinococcota
Pisuviricota
Bacillota
Euglenozoa
Pseudomonadota
Bacteroidota
Euryarchaeota

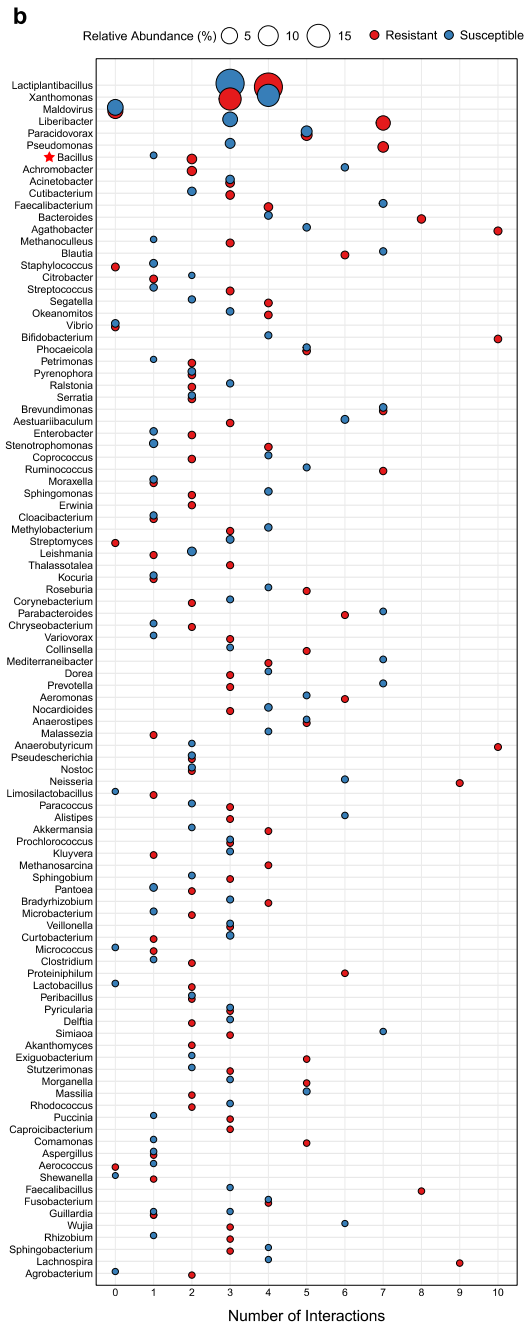
b
Relative Abundance (%) 5 10 15
Resistant
Susceptible
Lactiplantibacillus
Xanthomonas
Maldovirus
Liberibacter
Paracidovorax
Pseudomonas
Bacillus
Achromobacter
Acinetobacter
Cutibacterium
Faecalibacterium
Bacteroides
Agathobacter
Methanoculleus
Blautia
Staphylococcus
Citrobacter
Streptococcus
Segatella
Okeanomitos
Vibrio
Bifidobacterium
Phocaeicola
Petrimonas
Pyrenophora
Ralstonia
Serratia
Brevundimonas
Aestuariibaculum
Enterobacter
Stenotrophomonas
Coprococcus
Ruminococcus
Moraxella
Sphingomonas
Erwinia
Cloacibacterium
Methylobacterium
Streptomyces
Leishmania
Thalassotalea
Kocuria
Roseburia
Corynebacterium
Parabacteroides
Chryseobacterium
Variovorax
Collinsella
Mediterraneibacter
Dorea
Prevotella
Aeromonas
Nocardioides
Anaerostipes
Malassezia
Anaerobutyricum
Pseudescherichia
Nostoc
Neisseria
Limosilactobacillus
Paracoccus
Alistipes
Akkermansia
Prochlorococcus
Kluyvera
Methanosarcina
Sphingobium
Pantoea
Bradyrhizobium
Microbacterium
Veillonella
Curtobacterium
Micrococcus
Clostridium
Proteiniphilum
Lactobacillus
Peribacillus
Pyricularia
Delftia
Simiaoa
Akanthomyces
Exiguobacterium
Stutzerimonas
Morganella
Massilia
Rhodococcus
Puccinia
Caproicibacterium
Comamonas
Aspergillus
Aerococcus
Shewanella
Faecalibacillus
Fusobacterium
Guillardia
Wujia
Rhizobium
Sphingobacterium
Lachnospira
Agrobacterium
0 1 2 3 4 5 6 7 8 9 10
Number of Interactions

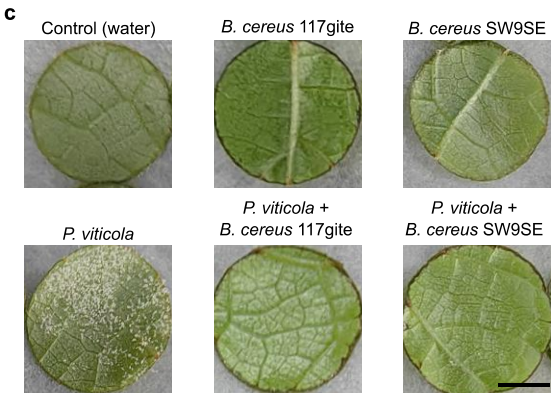
c
Control (water)
B. cereus 117gite
B. cereus SW9SE
P. viticola
P. viticola + B. cereus 117gite
P. viticola + B. cereus SW9SE

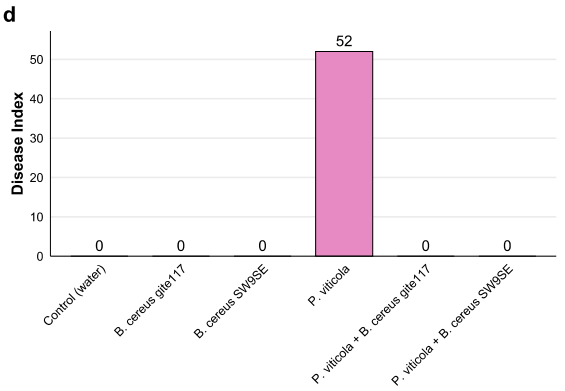
d
Disease Index
0
10
20
30
40
50
52
0
0
0
0
0
Control (water)
B. cereus gite117
B. cereus SW9SE
P. viticola
P. viticola + B. cereus gite117
P. viticola + B. cereus SW9SE

Fig. 5 Downy-mildew resistance shapes complex microbial interaction networks with key genera. a, Microbial co-occurrence networks based on the DM resistance types. The networks displaying the top 200 most abundant genera within each type. Node sizes indicate genera' relative abundances, with colors denoting different phyla as shown in bottom panel legend. Green edges represent positive correlations, while red edges indicate negative correlations between nodes. The top 10 abundant genera within each microbiome were labeled above corresponding nodes. **b**, Profiles of top 100 abundant key microorganisms in the DM-resistant grapevine microbiome, illustrating relative abundances and numbers of microbial interactions. Colored bubbles represent the profiles in the corresponding microbiome. The top 100 genera of the resistant microbiome which not present in the top 200 genera in the susceptible microbiome were not shown in the plot. Red star indicates a genus that experimentally isolated and validated in this study. **c**, Biocontrol assay of two *B. cereus* strains against *P. viticola* infection. The top and bottom rows show mono- and co-inoculation, respectively. Black bar indicates 5 mm. **d**, Bar plot of the disease index shown in (**c**), where higher values indicate more severe infection.

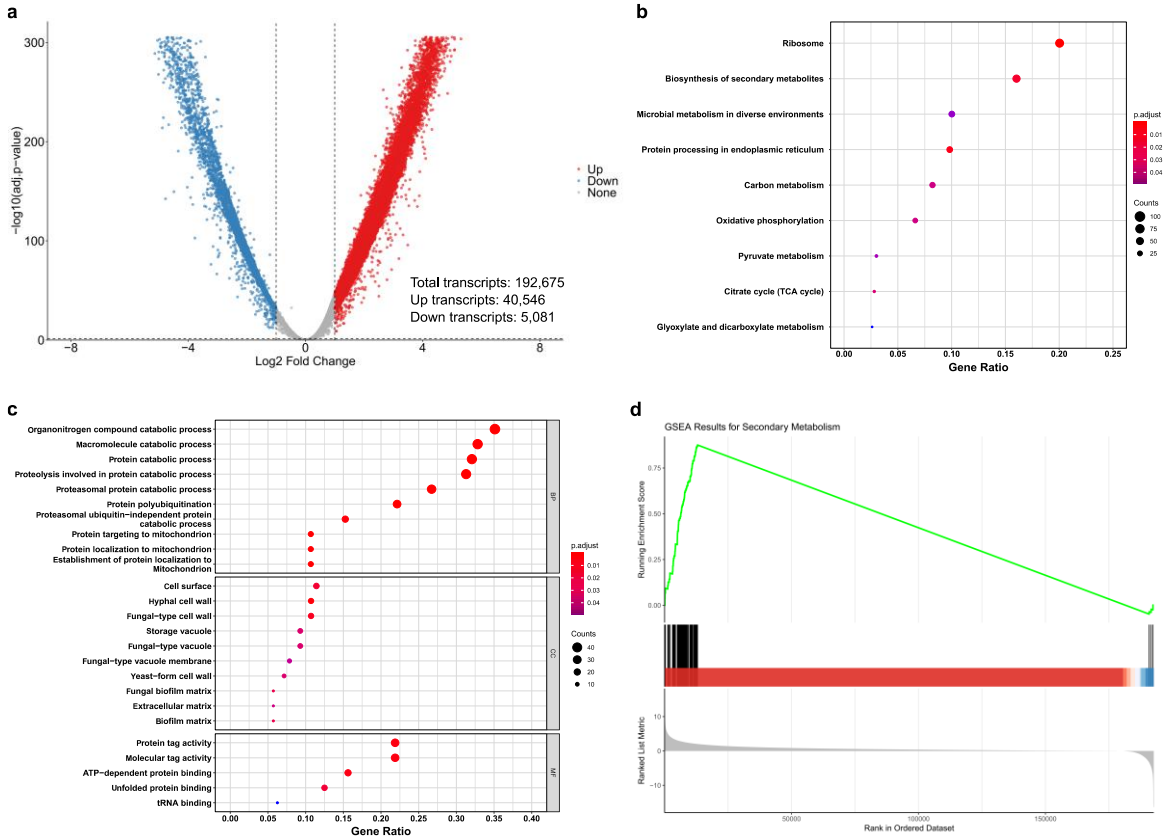

Fig. 6 Eukaryotic transcriptome profile of the grapevine phyllospheric microbiome in response to the oomycete *Plasmopara viticola* infection. a, Volcano plot of the grape microbiome upon infection by *P. viticola*. The dashed lines indicate thresholds for statistical significance (log2 fold change > 1, adjusted $p < 0.05$). **b-c**, KEGG pathway (**b**) and GO enrichment analysis (**c**) of the up-regulated DETs. GO enrichment shows the top 10 terms in each category. **d**, GSEA of the secondary metabolism-related transcripts. The graph illustrates the enrichment score (green line) for the transcript set associated with secondary metabolism across the ranked transcript list (bottom) by log2 fold change values. The black bars in the middle represent the positions of transcripts from the set in the ranked list with significances indicated by red and blue.

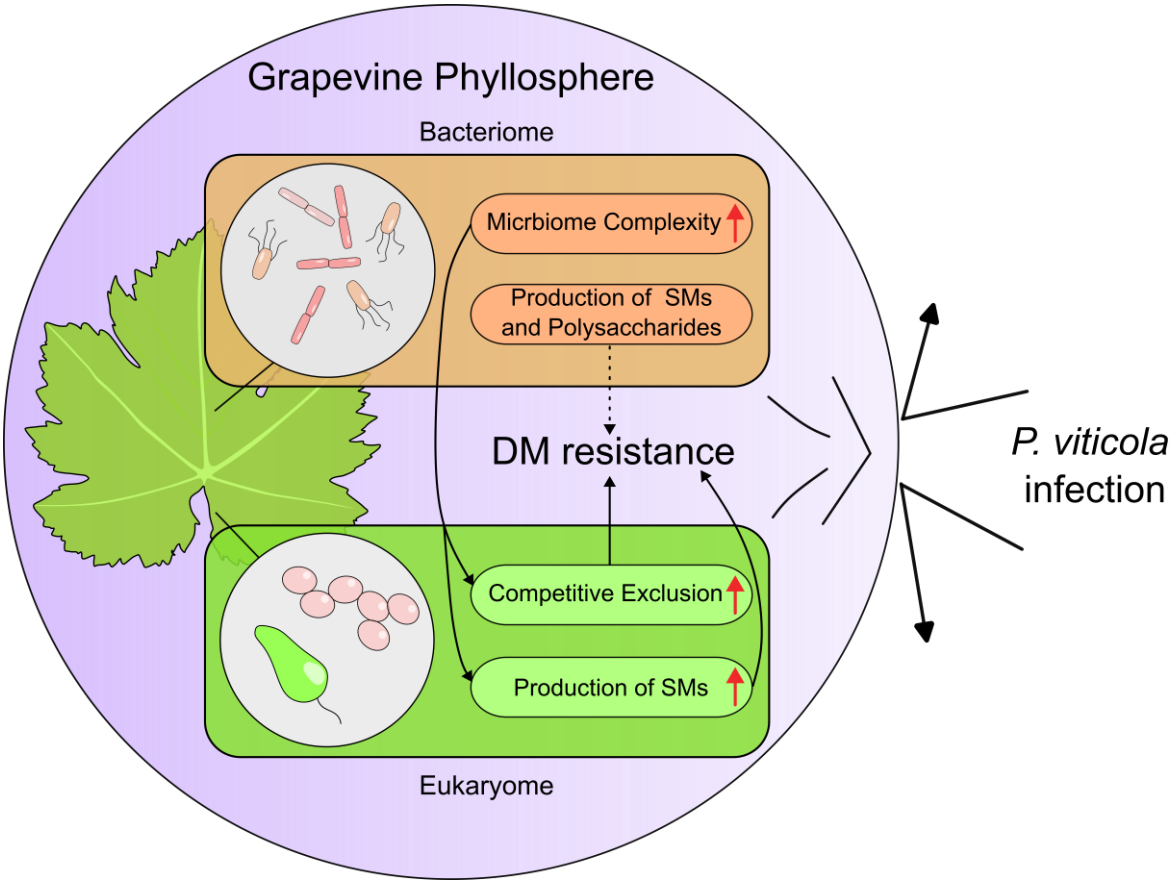

Fig. 7 Schematic diagram depicting the grapevine microbiome's potential deployment of bacteriome and eukaryome to combat *P. viticola* infection. This pan-metagenomic and pan-metatranscriptomic study demonstrates that the grapevine bacteriome orchestrates microbiome assembly, with key taxa (e.g., Bacillota) interacting selectively with eukaryotes (e.g., Euglenozoa) to mediate competitive exclusion and secondary metabolites (SMs). The bacteriome may further utilize SMs and polysaccharides for enhanced DM resistance (dashed line, speculative).

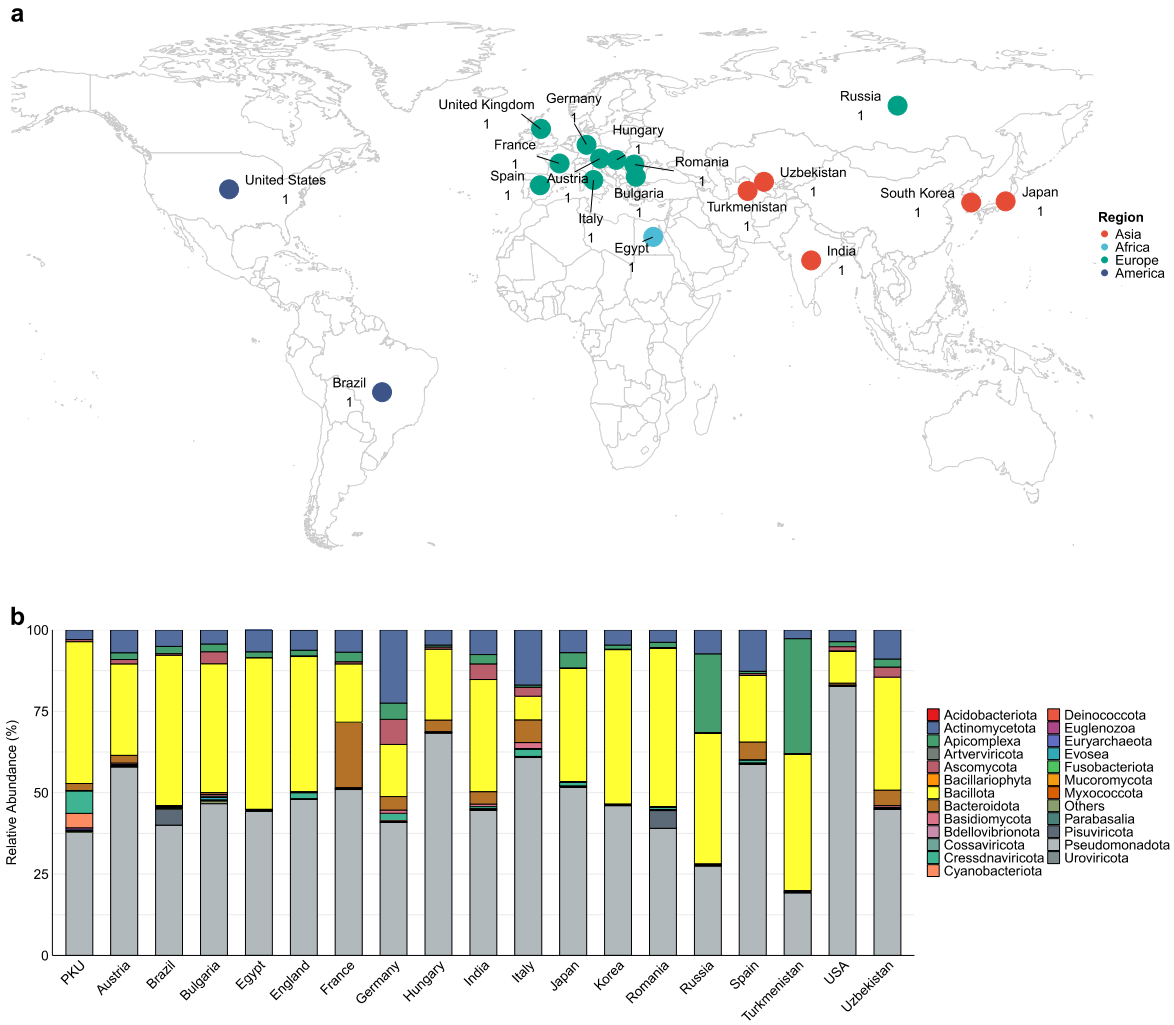

Fig. S1 Worldwide comparison of grapevine phyllosphere microbiome compositions. **a**, Geographical distributions of *Vitis* accessions used for comparative analysis. One representative *Vitis* accession was selected per country. **b**, Top 10 phylum level composition of grapevine phyllosphere microbiome across worldwide *Vitis* accessions. PKU represents mean phylum composition of this study.

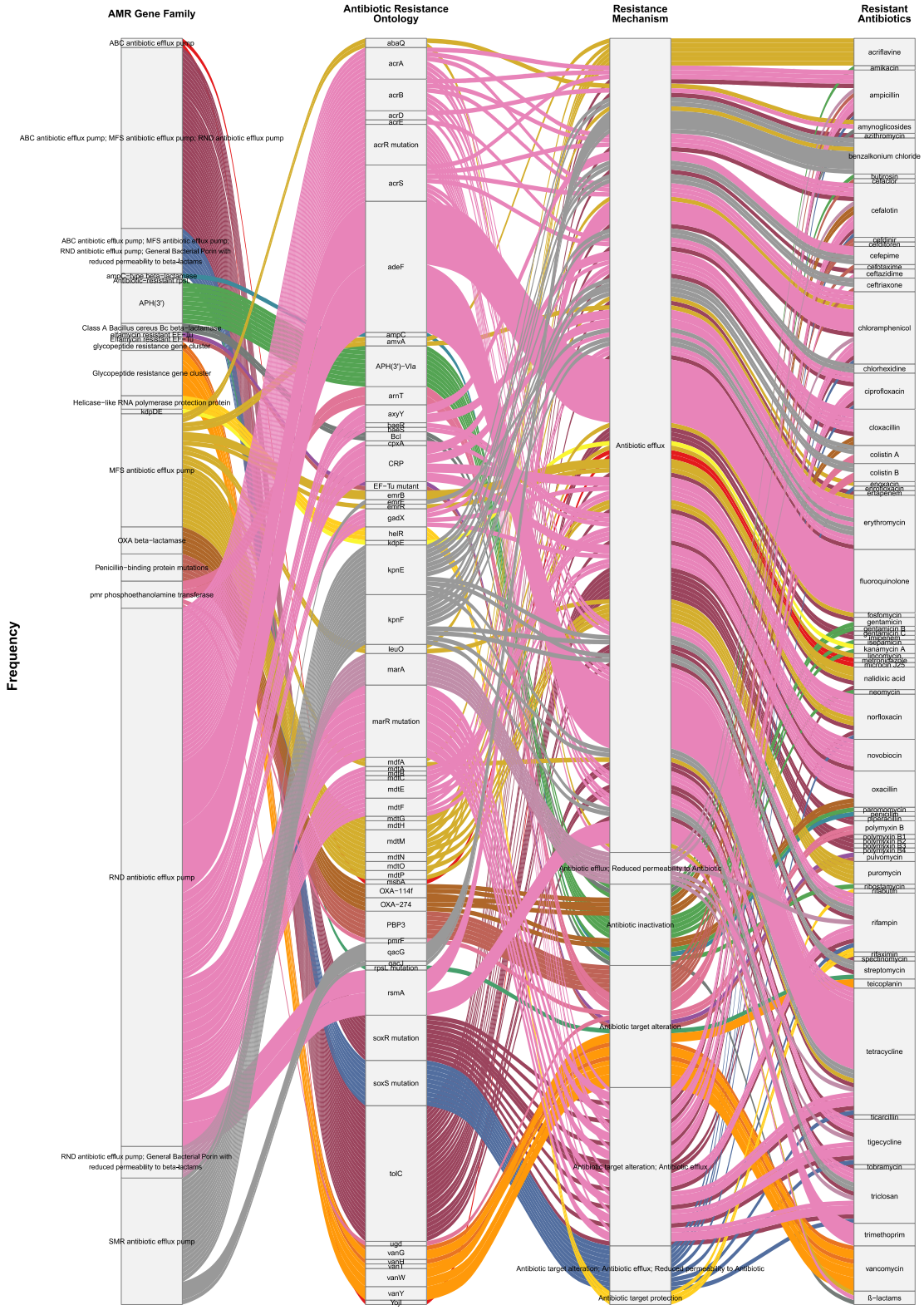

Fig. S2 Resistome profile of the GPMAGs. Identified AMR gene frequencies in the GPMAGs were categorized by gene family, resistance mechanism, and target antibiotics.

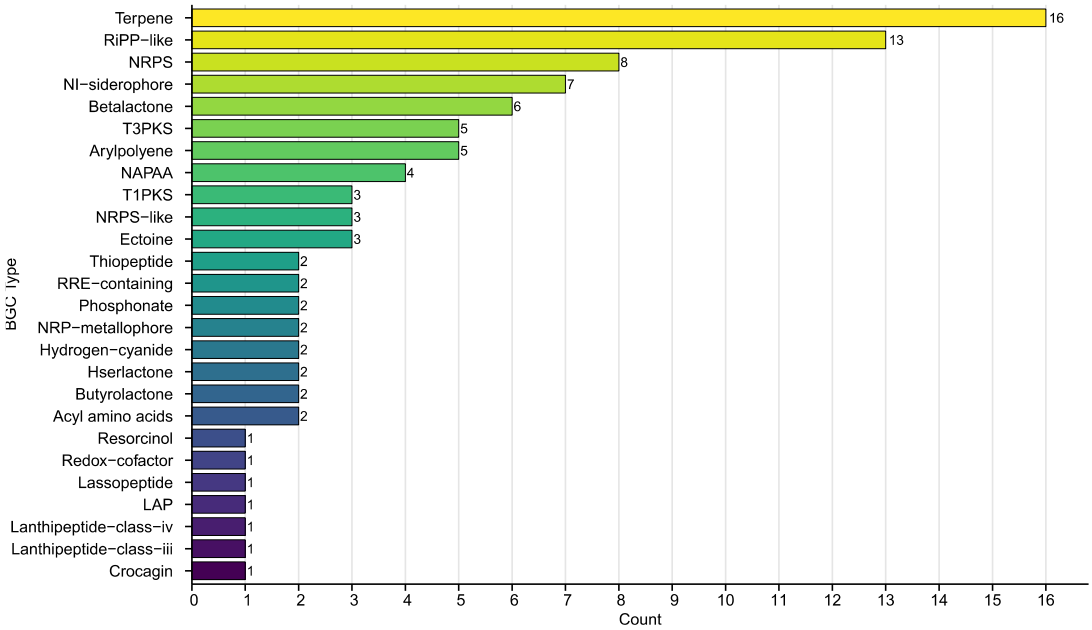

Fig. S3 BGC profile of the GPMAGs. Identified BGCs from the GPMAGs were displayed by bar chart.

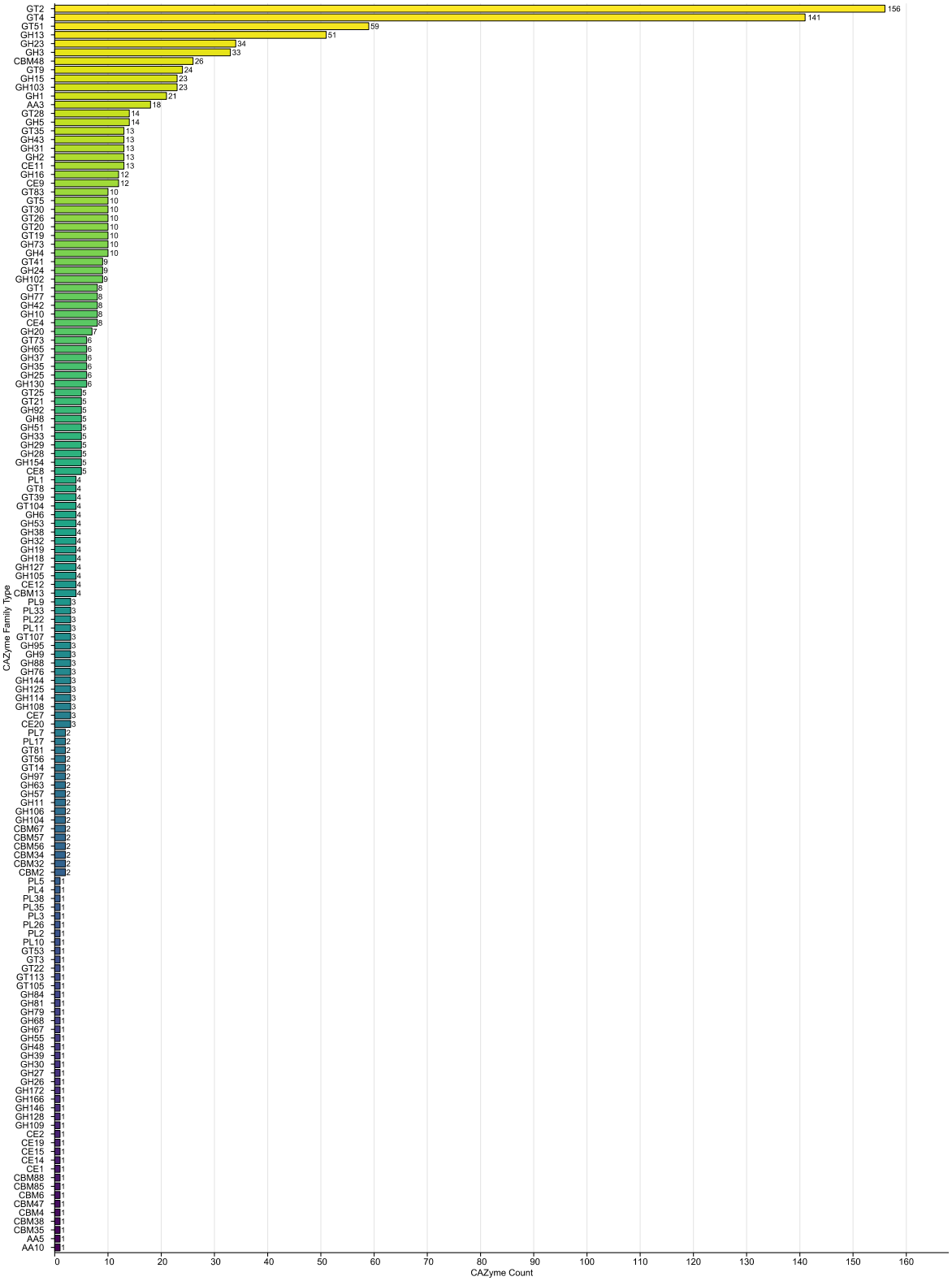

Fig. S4 CAZyme profile of the GPMAGs. Bar chart exhibits identified CAZyme types of the GPMAGs.

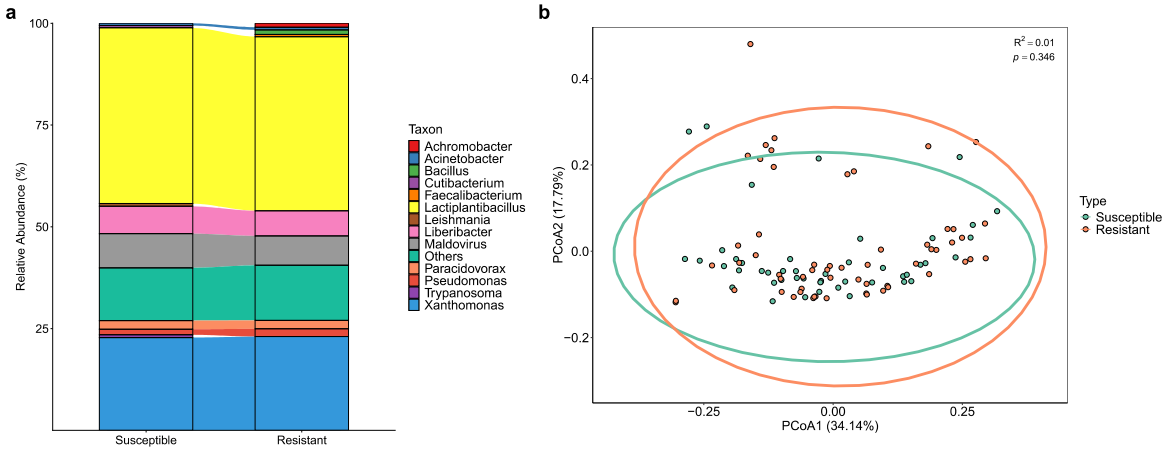

Fig. S5 Microbiome profiles associated with DM resistance. a, Mean relative abundances of the top 10 most abundant genera based on the types of DM resistance. **b**, PCoA of the grape microbiomes at genus level. Each point represents a grapevine accession with colored according to its variety. Ellipses denote the 95% confidence intervals for each group. Percentages on the axes indicate the variance explained by PCoA1 and PCoA2. PERMANOVA analysis revealed significant differences among the groups, with R^2 values represent the proportion of variance explained by the grouping factor and *p*-values indicate the statistical significance of these differences.

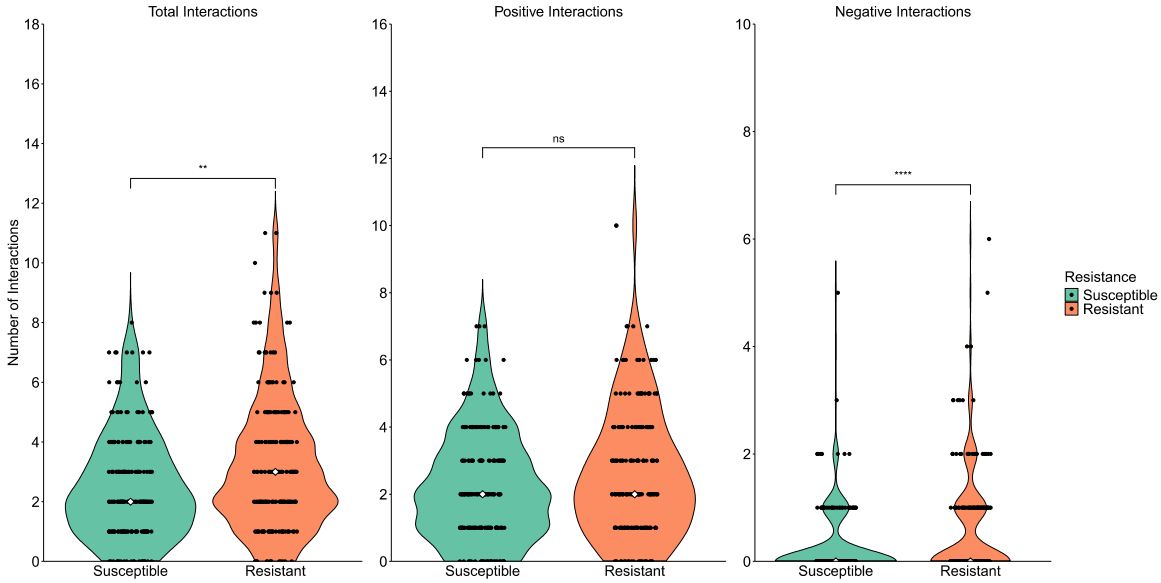

Fig. S6 Microbial interaction profiles associated with the DM-resistance. Violin plots depict the median microbial interactions for each node in the networks shown in Fig. 5a. White diamonds indicate medians for total interaction. Significance levels are denoted as ** ($p < 0.01$), **** ($p < 0.0001$), and ns (not significant).

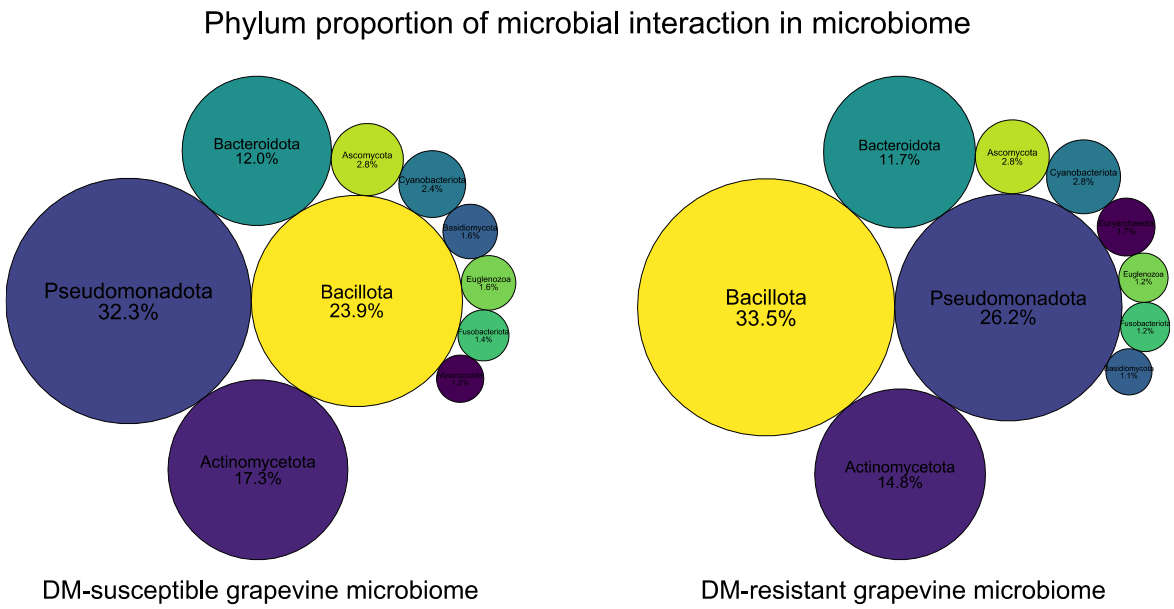

Fig. S7. Phylum-level microbial interaction proportions between microbiomes. Bubble plots display interaction frequencies among the top 10 abundant phyla in the susceptible and resistant microbiomes, with bubble sizes corresponding to proportional values (numerically labeled).

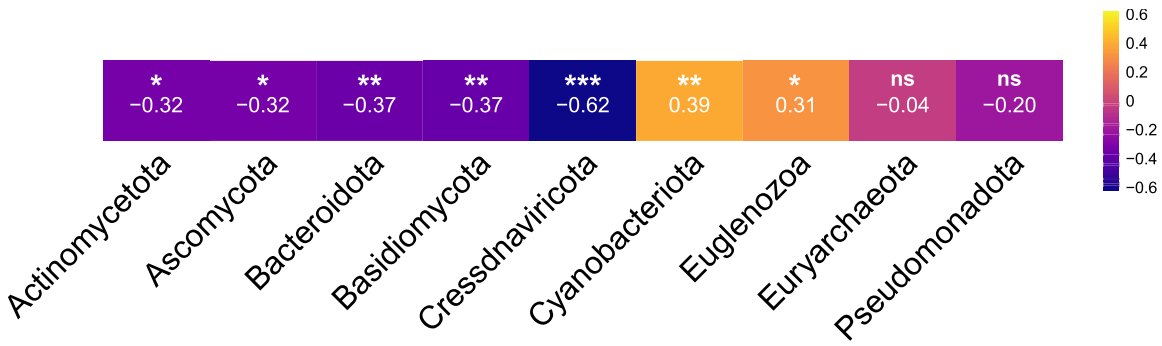

Fig. S8 Abundance correlation between Bacillota and major phyla in the resistant microbiomes. Heatmap depicts Spearman coefficients between Bacillota and major phyla based on their abundances in the resistant microbiome. Numerical values and significance levels * ($p < 0.05$), ** ($p < 0.01$), *** ($p < 0.001$), ns (not significant) are shown in cells.